Handbook of Research on Heterogeneous Next Generation Networking:
Innovations and Platforms

Stavros A. Kotsopoulos
University of Patras, Greece

Konstantinos G. Ioannou
University of Patras, Greece

Information Science REFERENCE
INFORMATION SCIENCE REFERENCE
Hershey · New York

Director of Editorial Content:	Kristin Klinger
Director of Production:	Jennifer Neidig
Managing Editor:	Jamie Snavely
Managing Development Editor:	Kristin M. Roth
Assistant Managing Editor:	Carole Coulson
Typesetter:	Chris Hrobak
Editorial Assistant:	Rebecca Beistline
Cover Design:	Lisa Tosheff
Printed at:	Yurchak Printing Inc.

Published in the United States of America by
Information Science Reference (an imprint of IGI Global)
701 E. Chocolate Avenue, Suite 200
Hershey PA 17033
Tel: 717-533-8845
Fax: 717-533-8661
E-mail: cust@igi-global.com
Web site: http://www.igi-global.com

and in the United Kingdom by
Information Science Reference (an imprint of IGI Global)
3 Henrietta Street
Covent Garden
London WC2E 8LU
Tel: 44 20 7240 0856
Fax: 44 20 7379 0609
Web site: http://www.eurospanbookstore.com

Library of Congress Cataloging-in-Publication Data

Handbook of research on heterogeneous next generation networking : innovations and platforms / Stavros Kotsopoulos and Konstantinos Ioannou, editors.

p. cm.

Includes bibliographical references and index.

Summary: "This book presents state-of-the-art research, developments, and integration activities in combined platforms of heterogeneous wireless networks"--Provided by publisher.

ISBN 978-1-60566-108-7 (hardcover) -- ISBN 978-1-60566-109-4 (ebook)

1. Wireless communication systems. 2. Heterogeneous computing. 3. Computer networks. I. Kotsopoulos, Stavros, 1952- II. Ioannou, Konstantinos, 1975-

TK5103.2.H3368 2009

004'.35--dc22

2008016294

British Cataloguing in Publication Data
A Cataloguing in Publication record for this book is available from the British Library.

Chapter XV
Simulation of Small-Scale Fading in Mobile Channel Models for Next-Generation Wireless Communications

Stelios A. Mitilineos
National Center for Scientific Research, "Demokritos," Greece

Christos N. Capsalis
National Technical University of Athens, Greece

Stelios C.A. Thomopoulos
National Center for Scientific Research, "Demokritos," Greece

ABSTRACT

Small-scale fading strongly affects the performance of a radio link; therefore radio channel simulation tools and models are broadly being used in order to evaluate the impact of fading. Furthermore, channel simulation tools and models are considered to be of utmost importance for efficient design and development of new products and services for Next Generation (Wireless) Networks (NGNs and NGWNs). In this chapter, a brief description of the most popular and broadly accepted mobile radio channel models and simulation techniques is given, mainly with respect to small-scale fading. In addition, certain research results on radio channel simulation are presented. The authors hope that the information provided herein will help researchers to acquire an insight to small-scale fading simulation techniques, which will be useful for a solid understanding of the underlying physical layer properties of NGWNs.

I. INTRODUCTION

According to the ITU definition [ITU, 2004], a Next Generation Network (NGN) is principally an heterogeneous network. NGNs are packet and IP-based networks, able of providing services (such as navigation or telecommunications services) using multiple broadband transport technologies, while service-related functions are independent from the underlying transport technologies. A user of a NGN enjoys different services from different providers seamlessly, anytime, anywhere (ubiquitous computing – ubiquitous communications). From a business-oriented point of view, NGNs will allow unrestricted access by users to different service providers; a specification that is expected to bring revolutionary effects to business models and functionality of all information and communication technology (ICT) enterprises. One of these effects is the already noticed unification of business sectors that were separated until now, like fixed and mobile telephony, internet and entertainment. From the user point of view, this means that she will be able of watching a streaming-video movie or placing a transatlantic call through a unique internet provider, or watching the weather forecast and hear her favourite songs from her mobile phone on the way to work. Furthermore, NGNs will naturally comply with all current and future regulatory requirements, regarding e.g. emergency communications (E-112 or E-911 for E.U. and U.S.A. respectively), or security and privacy/ethical issues, etc.

The heterogeneity of NGNs consists in services as well as physical networks. NGNs will offer a wide range of services, from relatively simple voice telephony and data transfer, to more demanding applications like streaming video, virtual private networks, public network computing or unified messaging. Furthermore, several futuristic services have been proposed like interactive and location-based gaming, distributed virtual reality, remote home/office management etc. The ultimate goal is nowadays considered to be the full integration of navigation and communications networks in order to provide exotic new services to end users [Ruggieri, 2006]. On the other hand, as long as physical networks are concerned, NGNs will comprise of lines ranging from simple PSTN to DSL broadband in wired cases, and from 2G to 4G cellular or WLAN, WiMAX, Wireless Sensor Networks, and other more exotic ones like interplanetary internet [Akan 2004], in wireless cases. This means that NGNs will be capable of seamlessly internetworking through legacy and broadband networks and will be characterized by generalized mobility. So far, the only means of achieving these goals is considered to be an all-IP approach, i.e. using the IP protocol in order to interconnect the most diverse devices and networks; therefore NGNs are often referred to all-IP networks as well, while the IPv6 protocol is expected to significantly contribute towards this direction (Dixit, 2006). At the same time, the most attractive physical layer means of implementing NGNs is via wireless infrastructure and/or ad-hoc networks (Next Generation Wireless Networks, NGWNs) in conjunction with gigabit-per-second order throughput wired infrastructures. Even in the case of wired NGNs, digital content is expected to be delivered to the end user via mobile handheld devices (mobile phones, palmtops, VoIP wireless phones etc.).

The critical finding regarding the wireless nature of NGNs is the main motivation for writing this chapter. It is more than evident that, since NGNs will basically consist of wireless and mobile networks, it is critical for engineers and researchers to obtain a solid understanding of the underlying wireless propagation medium of digital content delivery. Certainly, the wireless propagation channel is a very broad field of research, therefore we shall mainly hold back to small-scale fading attributes, which strongly affect the performance of a radio link. A presentation of the most popular and broadly accepted mobile radio channel models will be given, with respect to small-scale fading. On the other hand, it is also critical to be able to evaluate the performance of a telecommunications system under design or development. Analytic formulas for the calculation of critical channel characteristics are not available or are difficult to be extracted for state-of-the-art or beyond state-of-the-art radio channel models; therefore, simulation arises as the main tool for design and development. Therefore, the principles of small-scale fading simulation will be discussed and a number of simulation techniques and tools will be presented. Finally, certain research results regarding channel simulation will be illustrated. The authors hope that the information provided herein will help researchers to acquire an insight to small-scale fading simulation techniques, which will be useful for designing and developing NGWNs.

II. SIMULATION: DEFINITIONS AND CATEGORIZATION

Simulation may be defined as artificial reality, i.e. that research field whose intention is to mimic one or more attributes of reality (Jeruchim, 1992). The means of simulation, or simulation platform, is usually (and hereinafter) considered to be a computer system.

The complexity of communications and signal processing systems, as well as the increasing demand for telecommunications services, has led to significant efforts in order to accelerate *and* reduce the cost of the design and development of new products and services. Simulation is proposed as a useful approach which can allow the testing of brainstorming results and design proposals before a prototype is implemented or put to production line. Furthermore, simulation may offer a reference platform, which may be used in order to compare different techniques and algorithms, such as modulation techniques, smart antennas convergence algorithms, adaptive equalization algorithms, multiple access schemes, BER, diversity receivers, transmission strategies and other (Kotsopoulos, 2000; Karagiannidis, 2005; Sagias, 2005; Bithas 2007; Toumpakaris 2007). Another one of the advantages of using simulation is the large cutoff in resources spent in all stages of development. Therefore, it is not surprising that the simulation of telecommunications systems is widespread, and that the research and industry communities spend a large amount of time and money in order to develop efficient simulation tools.

The evaluation of a proposed solution may be accomplished via closed-form equations or numerical calculations, simulation, and implementation and measurement of a prototype. In practice, it usually comes out that an optimum combination of these three approaches must be followed. More specifically, closed-form equations may be used in order to assess a large number of candidate solutions during initial design stages. Of course, the assessment of complex systems and techniques is impossible by using equations and numerical calculations only. Therefore, during the middle design stages, simulation may be used in order to evaluate the most promising solutions. In these stages, simulation models are used that mimic the reality to the desired degree of complexity. In final stages, a prototype may be implemented and measured. Usually, a closed loop of simulation, prototype implementation and measurement, revision, re-calculation, re-implementation and so on is established until the desired outcome is reached.

In all cases, system designers' attention must be pointed out to the desired degree of detail in representing reality. In many applications, the exaggerated request for detailed representation will render the simulation time enormous without offering any advantages with respect to the simulation subject of research. Simulation time, which is the time needed in order to complete the simulation of a system, is the main criterion for evaluating a simulation tool – along with the accuracy of results of course!

The models and techniques for channel simulation are herein divided into three broad categories: in-situ measurements models, statistical and geometric models, and deterministic models. In the literature, there is an ambiguity with respect to statistical models (usually referred to as empirical models as well). Some authors consider that statistical modeling is the procedure of channel measurement for various transmitter-receiver placements and probability curve fitting to the experimental data. Others consider statistical modeling as arising from a geometric channel description which concludes to a statistical model. In fact, a statistical model that arises from a geometric description may be validated via measurements. On the other hand, a measurements campaign usually ends up with a statistical model, but this model does not correspond to a natural or geometric description or attribute of the channel, but rather is a best-curve fitting procedure. As an example, consider the Okumura-Hata model for the mean attenuation in macrocells (Okumura, 1968; Hata, 1980), or the Weibull PDF for the time interval between pulses time of arrival in wideband channel models (Yegani, 1991).

Herein, we adopt the assumption that channel measurements and curve fitting are categorized as in-situ measurements based modeling. On the other hand, we consider statistical modeling as either the direct utilization of PDFs for various channel attributes, such as Direction-of-Arrival (DoA), signal strength, Doppler spread and Doppler spectrum, etc., or the utilization of geometric channel models which are used in order to extract a desired channel attribute's PDF. Theoretical distributions often need to be validated via in-situ measurements, but this discrimination is used for clarity. Finally, there is another channel modeling category used, namely deterministic channel modeling (also referred to as site-specific propagation prediction). In this case, topographical maps or architectural plans of a specific site are used and conclusions are drawn up for the channel based on these data. Again, a deterministic model may be validated by in-situ measurements or a statistical model and so on. Finally, we consider that the objective of all types of modeling is the extraction of a statistical description of the radio channel with appropriate PDFs.

The discrimination among channel models to three broad categories is applied not only to mean attenuation but to small and large scale fading models as well, e.g., the mean attenuation may be calculated by in-situ measurements in a specific site. The experimental data may then be approximated by closed-form PDFs. For that reason, one of the available mean attenuation models may be utilized, e.g. Okumura-Hata models (Okumura, 1968; Hata, 1980), Lee models (Lee, 1986), etc. On the other hand, in-situ measurements may be avoided (with the respective impact to accuracy), and various statistical models be used instead. Finally, topographical maps and propagation prediction tools may also be used.

Similar procedures may be followed during large scale fading modeling. A possible statistical model in this case is that of Gudmundson (Gudmundson, 1991). However, as long as the deterministic modeling of large scale fading is concerned, this requires more detailed topographical data and larger resolution than in the mean attenuation case.

Finally, as long as small scale fading is concerned, various statistical properties may be calculated via in-situ measurements. These include Doppler, delay and angle spread, coherence time, bandwidth and distance, level crossing rate, average fade duration, etc. Also, it is possible to extract PDFs regarding the power and the complex envelope amplitude of the signal, the delay of arrivals, etc. Furthermore, it is possible to use geometric models or a priori PDFs in order to model fading. On the other hand, deterministic models have not yet been extensively used in order to model small scale fading, due to large detail depth and resolution of the digital representation of the actual environment that are required. Also, it is not easy to extract statistical conclusions regarding the effect of furniture, people moving around, etc., since the simulation time may become prohibitive for large and complex environments. Nevertheless, the ever growing computational power offers the possibility to present deterministic modeling solutions for small scale fading, as will be described later, but always under the constraint that the environment models are kept simple. In order for more complex environments, statistical analysis is proven more useful and is used more often in practical cases.

III. CHANNEL MEASUREMENTS

In-situ measurements may be performed in order to model a specific site. Depending on whether the signal measured is narrowband or wideband, mobile channel measurements deal with different channel and signal attributes. Narrowband signal measurements are usually related to frequency flat fading, while the ideal narrowband signal is an unmodulated carrier. To the contrary, wideband signal measurements usually refer to frequency selective fading, while the ideal wideband signal is a delta impulse function.

In narrowband signal measurements, it is usually the mean attenuation and power fluctuations that are of concern. Narrowband measurements and models do not offer information about the distribution of the delay of arrival or the power-delay profile, since it is considered that the respective delay differences are very small. They rather offer a statistical characterization of signal phase and Doppler shifts of the incoming signal components. As a result, they are used in order to calculate the attenuation factor β, the rms Doppler spread v_{RMS}, the PDF of the signal envelope, the level crossing rate and fade duration, etc. Then, the envelope's PDF may be used in order to calculate the Bit Error Rate (BER), Doppler spread may be used in order to calculate the level crossing rate, etc. Narrowband measurements are implemented by transmitting an unmodulated carrier and using appropriate measuring instruments, which have the capability of performing repetitive measurements with a high refresh rate (Pahlavan, 1995).

To the contrary, wideband measurements are mainly used in order to characterize the phenomenon of multipath fading itself. Using this type of measurements, we can calculate the number of different paths of the incoming signal components, the delay and mean power of each path (component), as well as the power PDF for each path. Thus, wideband measurements do rather simulate the delay distribution and power-delay profile, i.e. essentially the impulse response of the channel. The impulse response is measured either directly, by transmitting a very narrow pulse in the time domain (ideally a delta signal) and sounding the channel, or by measuring the frequency response of the channel for a large bandwidth and then calculating the impulse response via inverse Fourier transform (usually Inverse Fast Fourier Transform – IFFT). In any case, the achieved resolution is inversely proportional to the bandwidth of the transmitted signal.

An alternative method for measuring the impulse response is based on transmitting an inherently wideband pseudo-random sequence, such as a spread-spectrum sequence (e.g. direct-sequence spread spectrum), and then calculating the correlation of the received and transmitted signal. The result will be the channel impulse response. If the duration of each sequence chip (a "chip" is herein the "bit" of the pseudorandom signal modulating sequence) is sufficiently small in order to obtain the desired resolution, and at the same time the sequence period is sufficiently large in order to be able to detect large delays, such a system may replace the direct pulse sounding method. This method is considered to be preferable in the case of wide area networks (PCS, macrocells) because it offers stronger coverage than the direct pulse sounding method. On the contrary, the direct pulse sounding method is considered to offer better resolution, and thus it is preferred in small area networks (WLANs, micro- and pico-cells) (Pahlavan, 1995).

The interested reader may refer to the literature, where there have been reported interesting results regarding channel measurements and statistical modeling by various researchers, such as Alexander (Alexander, 1982), Saleh and Valenzuela (Saleh, 1987), Rappaport (Rappaport, 1989), Pahlavan et al. (Pahlavan, 1989), Hashemi and Tholl (Hashemi, 1994), Kim et al. (Kim, 1996), and other.

IV. GEOMETRIC MODELS

Geometric models are based on abstract geometric characteristics of the propagation environment, which are common to mobile channels of the same type. In essence, they are a subset of the statistical channel models category, since they inevitably end up to specific distributions for the angle of arrival, the power to angle of arrival distribution, the signal envelope etc. However, geometric models are of special importance, since they are based on the channel's natural characteristics and offer an intuitive insight to the channel propagation mechanisms. Some of the most popular geometric models are presented herein.

Ossana's Model

Ossana's model assumes a flat power spectrum and the existence of a LOS component between transmitter and receiver (Ossana, 1964). Thus, Ossana's model is not useful for the majority of cellular systems, where there usually exist NLOS conditions.

Clarke's Model

A broadly accepted model for small-scale fading is Clarke's model (Clarke, 1968), which results to Rayleigh type fading (it is also reported in the literature as GBSBCM model (Liberti, 1999)).

This model assumes the existence of a dense ring of scatterers surrounding the mobile receiver, as well as a uniform distribution for the angle of arrival and phase of each incoming component. The amplitudes of all incoming components are equal to one another (isotropical scattering). This model is presented in Figure 1, where it is assumed that $d_1 > r$. It can be used in order to model macrocell channels, such as GSM and outdoor environment systems, where the transmitter is placed at a much greater height than the receiver. Therefore, all scatterers are densely distributed around the receiver, while there is none or very few scatterers around the transmitter.

The signal envelope in this case is shown to follow a Rayleigh distribution, having the classic Doppler spectrum given by (Liberti, 1999; Stuber, 2001)

$$S_{rr}(v) = \begin{cases} \dfrac{\Omega_p}{4\pi v_m} \dfrac{1}{\sqrt{1-[(v-f_c)/v_m]^2}}, & |v-f_c| \le v_m \\ 0 & ,|v-f_c| \ge v_m \end{cases} \tag{1}$$

In the case of a Ricean type channel, the Doppler spectrum additionally includes a delta function with amplitude proportional to the K-factor, which function corresponds to the Doppler shift (and related to the angle of arrival) of the LOS component.

Furthermore, Figure 1 may be used in order to model the signal received by the Base Station (BS) (Jakes, 1994). In this case, the power to angle of arrival profile will be concentrated around the angle θ_1 (it is reminded that the principle of reciprocity should be carefully applied when it comes to the spatial characteristics of the wireless radio channel (Paulraj, 2003)).

Figure 1. Clarke's model for cellular systems

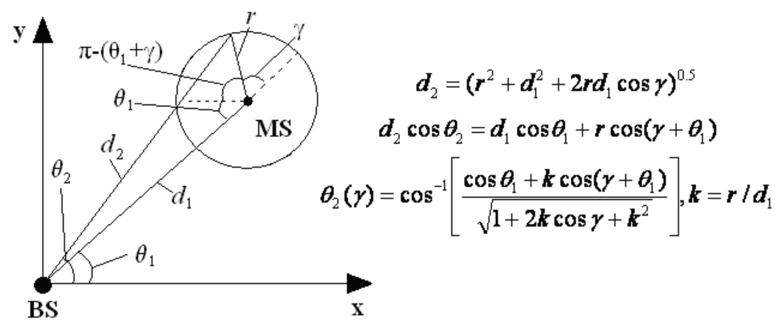

Elliptical Models

Elliptical models represent the radio channel by assuming that all scatterers are placed on one or more ellipses surrounding the transmitter and receiver, and that the foci of these ellipses coincide with the transmitter and receiver positions. A schematic representation of this category of models is shown in Figure 2. The elliptical models apply in cases where the transmitter and receiver have similar heights to one another, therefore the scatterers may be assumed to be placed densely around not only the receiver but the transmitter as well. These cases include micro- and pico-cell channels, such as indoor environment networks (e.g. WLANs etc.)

In the case of frequency flat fading, the differences among the delays of each signal component are negligible as long as the component's phase is *not* concerned. All scatterers may be modeled as being placed on an ellipse which surrounds both transmitter and receiver, as shown in Figure 2a. The main difference between this model and Jakes' model is that, despite the fact that the distribution of Angle-of-Departure (AoD) and power to AoD profile is uniform at the transmitter, the Angle-of-Arrival (AoA) and power to AoA distribution is not uniform at the receiver. Consequently, the Doppler spectrum is different than the one given by equation (1). Small differences in the scatterers placements on the ellipse result to large differences to the phase of the incoming component, therefore the phase of each component is still considered to be uniformly distributed.

In frequency selective channels, the scatterers are grouped to different ellipses, and the channel is modeled as the sum of multiple frequency flat channels, as shown in Figure 2b. In urban and suburban environments these ellipses may e.g. correspond to nearby scatterers like high buildings on the one hand, and faraway morphology characteristics like mountains etc. on the other hand. The ellipses are usually considered to be discrete, i.e. the model consists of a number of discrete ellipses, each of which corresponds to a different delay. This channel corresponds to a tapped delay line filter, as in Figure 3. This is due to the fact that all signals that are reflected from a particular ellipse arrive at the receiver having almost the same delay, no matter what the AoA or AoD are.

On the other hand, there are cases where a continuous ellipses assumption is more applicable, like in tropospheric scattering or some mobile channels. In this case, the model may also be represented by a tapped delay line filter, but the delays are now multiples of a differential delay as shown in Figure 4. In the case of digital systems with a sampling period of T_s, T_s being the symbol duration, it is usually suggested that $\Delta\tau = T_s$ (Stuber, 2001).

The GBSBEM Model

The GBSBEM model is an extension of the elliptical models, properly adapted for indoor environments (Liberti, 1996; Liberti, 1999). This model is characterized by the assumption of the existence of a large number of scatterers (in the ideal case there will be an infinite number of scatterers) which are uniformly distributed within an ellipse whose foci coincide with the transmitter and receiver positions, as shown in Figure 5. The size of the ellipse corresponds to the excess delay, which is the maximum delay observed in the channel. The scatterers are grouped to differential ellipses, which on the one hand are limited by the transmitter-receiver Line-Of-Sight (LOS) and

Figure 2. Elliptical geometric models configuration for frequency flat and frequency selective channels

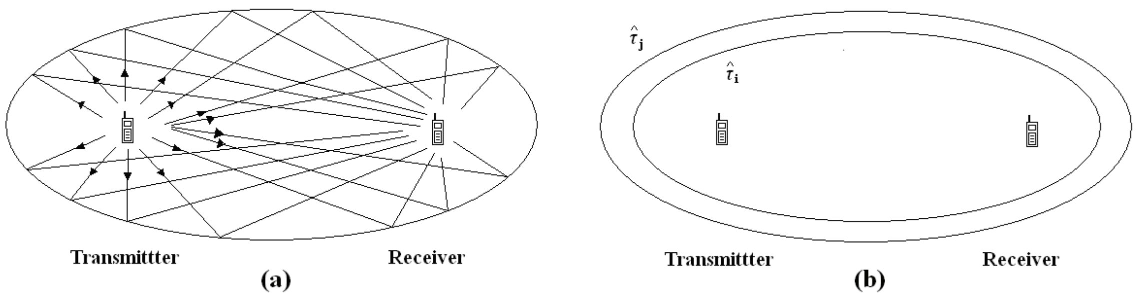

Figure 3. Discrete tapped delay line filter for the simulation of a frequency selective radio channel

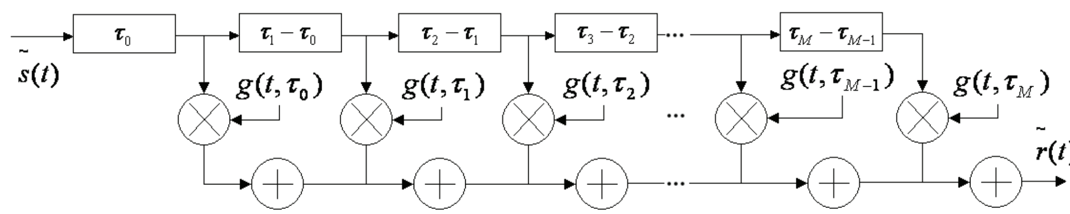

on the other hand are limited by the external boundary-ellipse. Furthermore, all incoming signal components are assumed to arise after *one* reflection only. For these reasons, this model is named GBSBEM (Geometrically Based Single Bounce Elliptical Model).

Referring to Figure 5, the normalized delay $r_i = \tau_i/\tau_0$ is defined as the ratio of the delay of an incoming component versus the delay corresponding to the LOS between transmitter and receiver. The maximum normalized delay is given by $r_m = \tau_m/\tau_0$. A way of calculating the maximum normalized delay is to set a threshold of the received power, e.g. *T*dB below the LOS component power, below which any received power may be considered to negligible. Then, the maximum normalized power is given by (Liberti, 1999)

$$r_m = 10^{\frac{T-L_r}{10n}} \tag{2}$$

where L_r represents the loss due to one scattering and n is the propagation attenuation factor.

Other Models

The following are cited some other popular geometric models. The interested reader may further refer to the informative works of Ertel et al. (Ertel, 1998), as well as Liberti-Rappaport (Liberti, 1999), but also to newer results included in the work by Sarkar et al. (Sarkar, 2002).

Lee's model is an extension of Clarke's model, where the scatterers are discrete and uniformly distributed around the mobile receiver (Lee, 1982). The main difference between this model and Clarke's model is that the scatterers have a discrete rather than a continuous distribution. Stapleton's model is a further extension of Lee's model, where it is additionally assumed that the scatterers have an angular velocity with respect to the receiver, while more than one ring of scatterers are considered (Stapleton, 1994; Stapleton, 1996). Another extension of Lee's model is Aszetly's model, where the scatterers occupy a sector rather than a whole ring. Also, Norklit's or Uniform Sector Distribution (USD) model should be mentioned, which is characterized by a uniform distribution of scatterers within a disc sector (Norklit, 1994).

Figure 5. A geometric representation of the GBSBEM model

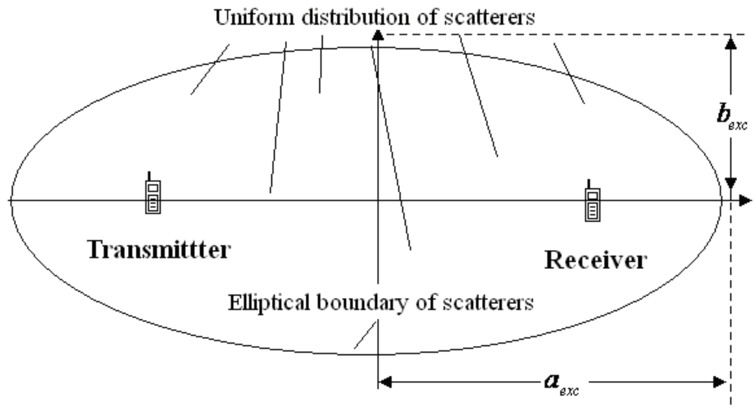

Figure 4. Continuous tapped delay line filter for the simulation of a frequency selective radio channel

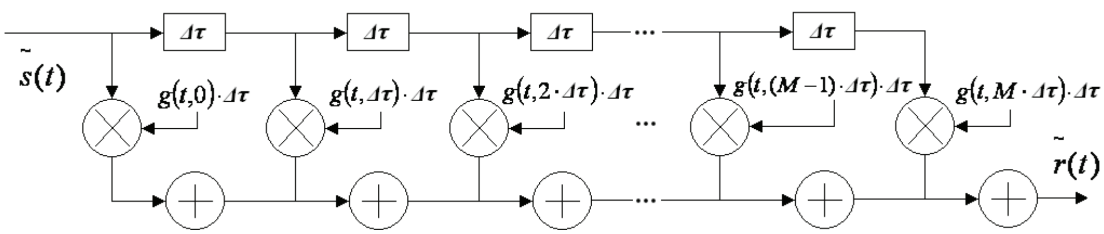

Furthermore, there are some popular models for cellular systems, namely the Typical Urban (TU) and Bad Urban (BU) models, as well as JTC and COST models (JTC, 1994; COST207, 1986). According to the TU model, a number of 120 scatterers are uniformly distributed within a circular disc of 1km radius centered at the Mobile Station (MS). The scatterers are assumed to be fixed as the MS moves for 5m, and then their relative positions to the MS are restored. In each 5m window, it is assumed that the incoming signal components are characterized by uniformly distributed phase and large scale fading with a standard deviation of 5-10dB. This model concludes to AoA distributions of the Gaussian type, like the GAA model cited (Ertel, 1998).

The BU model is similar to the TU, but there is an additional cluster of 120 scatterers, placed at an angle of 45º with respect to the main cluster and the BS]. The signal power corresponding to the secondary cluster of scatterers is 5dB below that of the main cluster. Due to this secondary cluster, the angle and delay spread are increased.

According to the Gaussian WSSUS (GWSSUS) model, the scatterers are grouped to cluster surrounding the receiver, while for each cluster the delay is considered to be constant (Zetterberg, 1995; Zetterberg, 1996). Each cluster consists of a large number of scatterers, therefore the Centrali Limit Theorem (CLT) can be applied. Another version of the GWSSUS model is the Gaussian Angle of Arrival (GAA) model, where only one cluster of scatterers is considered, while the angle of arrival is Gaussian distributed with mean value the angle of observation of the specific cluster.

Raleigh's model assumes that multipath fading is caused by a small number of dominant scatterers (Raleigh, 1995). Similar assumptions are made by the Polydorou-Capsalis model (Polydorou, 1997). However, the Raleigh model also takes into account the effect of large scale fading.

Klein and Mohr's model (Kein, 1996) is an extension of the tapped delay line filter model, where discrete AoAs are determined too, and therefore it offers information for the AoA of each incoming signal component too. The Lu-Lo-Litva model is an elliptical-type model, according to which the scatterers are clustered to elliptical rings surrounding the transmitter and receiver, while the number of scatterers of each cluster follows a Poisson distribution (Lu, 1997). The Lotter and van Rooyen model is a statistical model which is based to geometric assumptions as well as relative measurements found in the literature (Lotter, 1999), and can be applied to cellular DS-CDMA systems incorporating smart antennas. Other models for the impulse response of wideband radio channels are the Rappaport-Seidel model for indoor environments (Rappaport, 1991) and the Huang model for outdoor environments (Rappaport, 1993).

In order to model the slow-term variations due to shadow fading and also incorporate small scale fading, two basic approaches have been proposed. The first one has been presented by Suzuki (Suzuki, 1977) and Hansen and Meno (Hansen, 1977), and is based on a Rayleigh with a lognormal process. The second one has been presented by Loo and resembles a Ricean model with the additional property that the LOS component is lognormally distributed; this concludes to a model that adds a lognormal and a Rayleigh process (Loo, 1985). Loo's model has been further extended by Karadimas and Kotsopoulos by incorporating a sectored arrival of multipath energy and a 3-dimensional propagation model (Karadimas, 2007).

V. STATISTICAL MODELS – SIMULATION OF FREQUENCY FLAT FADING

The simulation of a narrowband mobile channel using statistical models may be performed by several proposed techniques. A popular technique consists in white noise filtering, thus creating the desired Doppler spectrum of the fading signal. Another widespread technique consists in summing multiple unmodulated carriers, each of which having an appropriate Doppler shift and phase distribution. The arising fading signal should have a prescribed envelope distribution, AoA distribution, power to angle of arrival profile, or Doppler spectrum. This means that these distributions are generated according to the prescribed channel specifications and do not necessarily correspond to the distributions that arise by the geometric models illustrated in Figures 1 and 2.

Simulation of Frequency Flat Fading Using Filtered White Noise

A popular technique for implementing flat fading simulators is by white noise filtering in order to generate the in-phase and quadrature phase components of the flat fading signal, and then vector summing these components. In order to implement a simulation tool of this type, it is required to create a white noise generator, which is used in order to generate two white noise signal samples having a phase difference of $\pi/2$ between each other. Each sample is then filtered by a bandpass filter with an appropriate frequency response, and then the two samples are vector summed. It must be preserved that the phase of the final signal is uniformly distributed within $[0,2\pi]$. In Figure 6 the block diagram of a white noise filtering channel simulator is illustrated.

In order to simulate a signal of prescribed Doppler spectrum, it is required to implement a filter having appropriate frequency response. In the case where the Doppler spectrum is given by equation (1), i.e. the Doppler spectrum corresponds to isotropical scattering (Rayleigh envelope), it is proposed that the frequency response of this filter be similar to the one illustrated in Figure 7 (Pahlavan, 1995). In order to implement a prescribed Level Crossing Rate (LCR), the rms bandwidth of the filter should be set equal to (Pahlavan, 1995)

$$B_{Do-rms} = 0.678 \cdot LCR \tag{3}$$

In the case where a dominant LOS component exists (Ricean channel), it is sufficient to add an unmodulated carrier of appropriate frequency to the vector summed output of the simulator.

A major disadvantage of the white noise filtering technique is that an applicable filter should be of great order, therefore the simulation time is encumbered. Nevertheless, this technique may be used without modifications in order to create multiple fading signals, under the only constraint that uncorrelated noise generators are used. The feature of creating multiple fading signals is very useful when e.g. simulating MIMO channels.

Simulation of frequency flat fading using vector summed sinusoidal carriers – The Jakes model.

With the vector summed carriers method, the channel response (also referred to as fading signal (Harada, 2002) is directly created by using

Figure 6. Implementation of a white noise filtering channel simulator

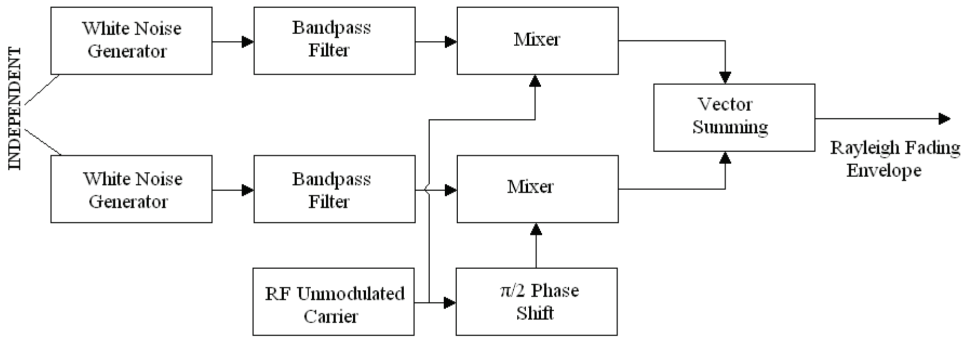

Figure 7. Frequency response of a filter required for the implementation of frequency flat small scale fading

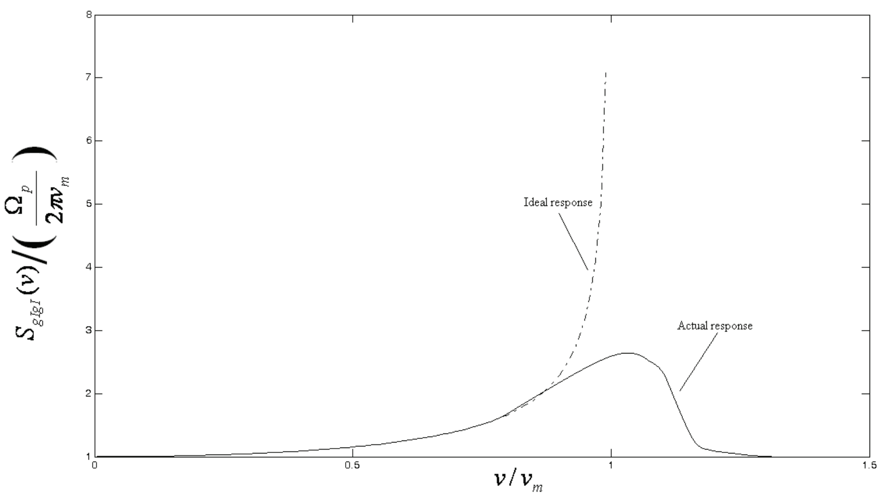

$$g(t,\tau) = \sum_{n=1}^{N} C_n(t)\exp(-j\varphi_n(t))\delta(\tau - \hat{\tau}(t)) = g(t)\delta(\tau - \hat{\tau}(t)) \tag{4}$$

$$\varphi_n(t) = 2\pi\{[f_c + v_{Do,n}(t)\pi_n(t)] - v_{Do,n}(t)\cdot t\} \tag{5}$$

where δ(.) is the Delta function, $\phi_n(t)$, $C_n(t)$,τ_n(t) are the phase, amplitude and delay of arrival of the *n*-th incoming component, $v_{Do,n}(t)$ is the Doppler shift of the *n*-th component, and f_c is the carrier frequency. Furthermore, since flat fading is considered, it comes out that $\tau_i - \tau_j \quad T_s, \forall i \neq j$, T_s being the symbol period. Therefore, it can be considered that $\tau_n(t) \approx \hat{\tau}(t)$ (the approximation $\tau_n(t) \approx \hat{\tau}(t)$ may not be used when calculating the phase of the incoming components, due to the large carrier frequency, which results to large phase differences even from small delay differences).

Using a normal distribution generator for creating AoAs, the result will approach the Doppler spectrum of Figure 7. Also, by directly adding a dominant component at the output, a Ricean channel simulator is easily implemented. Furthermore, when using equation (5), any prescribed Doppler spectrum may be incorporated.

Certainly, the phase of each component must be appropriately selected in order that the final simulator output signal exhibits uniform phase distribution.

Aiming to keep the number of incoming components small, Jakes proposed a model which requires significantly fewer incoming components (Jakes, 1974; Jakes, 1994). According to Jakes model, the signal envelope is given by

$$g(t) = \frac{\Omega_p}{\sqrt{2N_0+1}}[g_c(t) + jg_s(t)] \tag{6}$$

where

$$g_c(t) = 2\sum_{n=1}^{N_0}\cos(\varphi_n)\cos(\omega_n t) + \sqrt{2}\cos(\varphi_N)\cos(\omega_m t) \tag{7}$$

$$g_s(t) = 2\sum_{n=1}^{N_0}\sin(\varphi_n)\cos(\omega_n t) + \sqrt{2}\sin(\varphi_N)\cos(\omega_m t) \tag{8}$$

In the previous equations $\omega_n = \omega_m \cos(2\pi n / N_0)$ and $\omega_m = 2\pi v_m$, where v_m is the maximum Doppler shift. Furthermore, ϕ_n is the bias phase of the n-th component while ϕ_N is the bias phase of the component corresponding to the maximum Doppler shift.

For the purposes of a laboratory experiment, a carrier of desired frequency may be modulated by the envelope $g(t)$ given by equation (6). Alternatively, in the case of computer aided simulation, the fading signal of equation (6) is directly applied to the equivalent complex bandpass information-bearing signal.

According to Jakes, it is sufficient to use $N_0 = 8$ components, which correspond to $N = 2(2N_0 +1) = 34$ incoming signal components in equation (4) (Jakes, 1994). Nevertheless, equation (6) is not equivalent to equation (4). It has been proven that by using equations (7) and (8), the phases of the incoming signal components are correlated, which in turn implies that fading is not stationary (Pop, 1999; Pop, 2001). Evenmore, the envelope's autocorrelation when using Jakes model is significantly diverted from the theoretically predicted one for large time delays (Stuber, 2001). Pop and Beaulieu suggested an improved fading simulator based on Jakes model (Pop, 2001), however their simulation also generates second-order statistics that diverge to the theoretically predicted statistics. Moreover, it has been shown that this can not be corrected, not even in the case where $N_0 \to \infty$ (Chengshan, 2002). Pop and Beaulieu dealt with this issue and showed recently that the most efficient means of improving the statistical behavior of a fading simulator is to properly configure the output Doppler spectrum (Pop, 2002).

Simulation of frequency flat fading using vector summed sinusoidal carriers – Flat and Gaussian Doppler spectrum.

As already mentioned in the previous section, the Doppler spectrum may be given any desired shape. A case of special interest is the flat Doppler spectrum where,

$$S_{glgl}(f) = 1/2\pi v_m, |v| \le v_m \tag{9}$$

g_1 being the in-phase component of the channel response in equation (4).

Equation (9) corresponds to the case where the scatterers are placed with spherical symmetry around a constant velocity mobile receiver. The flat Doppler spectrum also applies to the case where the transmitter and receiver are fixed and there are scatterers moving around both of them in a stochastic manner, like in WLAN applications (Pahlavan, 1995).

In practical applications, the spectrum of equation (9) is implemented using either filtered white noise or by directly summing sinusoidal carriers like in equation (4). In the latter case, the sinusoidal carriers must have a Doppler shift that it uniformly distributed within the interval $[-v_m, v_m]$ rather than arising from the AoA distribution. This means the Doppler shift of each component is forced to follow a uniform distribution. Again, it is reminded that the components' phases in equation (4) must be appropriately selected in order that the output signal's phase is uniformly distributed.

Another case of Doppler spectrum shape with special interest is the Gaussian Doppler spectrum used in the COST207 model (COST207, 1986). In this model, the Gauss1 spectrum given by

$$S_{gIgI}(f) = G(A, -0.8v_m, 0.05v_m) + G(A_1, 0.4v_m, 0.1v_m), |v| \leq v_m \tag{10}$$

as well as Gauss2 model given by

$$S_{gIgI}(f) = G(B, 0.7v_m, 0.1v_m) + G(B_1, -0.4v_m, 0.15v_m), |v| \leq v_m \tag{11}$$

are used. In equations (10) and (11), $G(A, m, \sigma)$ is a Gaussian distribution with mean m, standard deviation σ and normalization factor A. Furthermore, $A_1\big|_{dB} = A\big|_{dB} - 10dB$ and $B_1\big|_{dB} = B\big|_{dB} - 15dB$. In practical cases, the Gaussian Doppler spectrum is implemented in a way similar to the flat Doppler spectrum described before.

Multiple Frequency Flat Fading Signals

A simulator is often required to be able to generate more than one fading signals, like in the case of simulating MIMO channels. The main objective in cases like this is to preserve that the multiple fading signals are uncorrelated to one another. Jakes proposed a modification to his technique, where a specific phase bias is added to each sinusoidal carrier, but this method can not deliver uncorrelated fading signals for time delays greater than zero (Stuber, 2001). An alternative solution is proposed by Dent et al, where it is suggested to use orthogonal Walsh-Hadamard codewords (Dent, 1993), which achieves a very low autocorrelation among the fading signals even for relatively large time delays.

Finally, in the case where it is desired to achieve a specific autocorrelation degree between two fading signals, it can be performed by a linear combination of two uncorrelated fading signals (Stuber, 2001).

VI. STATISTICAL MODELS—SIMULATION OF FREQUENCY SELECTIVE FADING

Frequency selective fading usually corresponds to wideband signals and channels. The simulation of frequency selective mobile channels using statistical models is based on the tapped delay line filters illustrated in Figures 3 and 4. The fading signal corresponding to each tap consists of a set of incoming components, is frequency flat and exhibits a specific envelope distribution, AoA distribution, power to AoA profile and Doppler spectrum. Furthermore, referring to Figure 8, we are also interested in determining the delay distribution of each incoming path as well as the distribution of the mean power with respect to the delay of arrival.

The time-variant nature of the radio channel should ideally be traced by sampling the impulse or frequency response of the channel with a rate equal or greater than two times the rms Doppler spread. (Pahlavan, 1995). In the case where the design of smart antennas or MIMO systems is of interest, then the distribution of the AoA of the main as well as subsequent paths, and the signal signature at the receiver should also be traced (Liberti, 1999), in order to evaluate whether or not a smart antenna would be able to trace successfully the time-variant characteristics of the radio channel.

Frequency selective fading modeling and simulation is performed either in the time or frequency domain, using the channel impulse response or frequency response respectively. Fourier theorem implies that these two techniques are equivalent to one another. In the following, some important aspects of time and frequency domain simulation are discussed.

Pulse Arrival Delay Distribution

A simple model for the time delay of incoming paths in wideband channels is the Poisson distribution, which is generally considered to be a good choice in the case where the scatterers are randomly placed around the receiver and transmitter (either for indoor or outdoor environments) (Pahlavan, 1995). Nevertheless, there are certain reports that the Poisson distribution does not sufficiently model the time delay of arriving paths (Turin, 1972; Suzuki, 1977; Yegani, 1991; Hashemi, 1993), which implies that the scatterers are not usually randomly placed around the receiver and transmitter. Ganesh and Pahlavan and Pahlavan and Levesque have dealt with this issue extensively in (Ganesh, 1989; Pahlavan, 1995).

Suzuki suggested an alternative time delay distribution (Suzuki, 1977), which was afterwards modified by Ganesh and Pahlavan for indoor environments (Ganesh, 1989), according to which the probability of a path incoming in a specific time window depends on whether a pulse arrived at the previous time window or not. It has been shown that this improved distribution approximates well enough the experimental data.

Furthermore, Saleh and Valenzuela suggested that all pulses in indoor environments arrive in clusters (Saleh, 1987). Each cluster's time delay is Poisson distributed, while the time delay of a specific pulse within a cluster also follows a Poisson distribution. This model also fits to the experimental data presented by Saleh and Valenzuela very well.

Furthermore, in a Poisson distribution the time intervals among the time delays of arrival are exponentially distributed. It has been suggested to replace the exponential distribution with other distributions, e.g. the Weibull distribution (Yegani, 1991); this approach may significantly improve the resulting accuracy of delay distribution estimation.

Pulse Amplitude Distribution for Each Path

It is broadly accepted that the pulse amplitude of each path suffers from flat fading, and more specifically follows the Rayleigh or Rice distribution, in the case where there exist NLOS or LOS conditions respectively. More specifically, it is considered that each path actually consists of more than one unresolvable paths. Thus, the wideband radio channel may be viewed as the sum of discrete narrowband radio channels with different time delays of arrival, as in Figure 2. The Doppler spectrum will be given by the appropriate equation, e.g. will be flat, Gaussian, Jakes or other.

Mean Path Power with Respect to Time Delay of Arrival

Ganesh suggested that the mean power of each path is exponentially distributed with respect to the time delay of arrival (Ganesh, 1991). This is a very important result, because it explicitly shows that the mean power of each path is exponentially declined with the time delay of arrival (of course, the instantaneous power still exhibits Rayleigh, Rice or other fading). More specifically, Ganesh calculated the mean power as the average within a small radius area rather than the average within a small time interval. It should herein be noted that this approach is correct only in the case where radio channel is homogeneous.

Models Given by Standards Committees

Standards committees suggest channel characteristics, which are then used as reference platforms in order to evaluate various methods and techniques, such as modulation schemes, adaptive filters and equalizers, link layer protocols, multiple access schemes etc. These standard characteristics usually include simulation models for large and small scale fading.

Referring to Figure 3, the suggested standards usually consist of tables in which the delays τ_i, as well as the mean values and PDFs of $g(t,\tau_i)$ are tabulated. Each table corresponds to a specific channel type. Certainly, the time delays are random and correlated, as well as time-variant. The same is valid for the amplitude and AoA of incoming components. Nevertheless, according to standards committees suggested models, all these character-

Figure 8. Impulse response snapshot for a wideband signal suffering from frequency selective fading

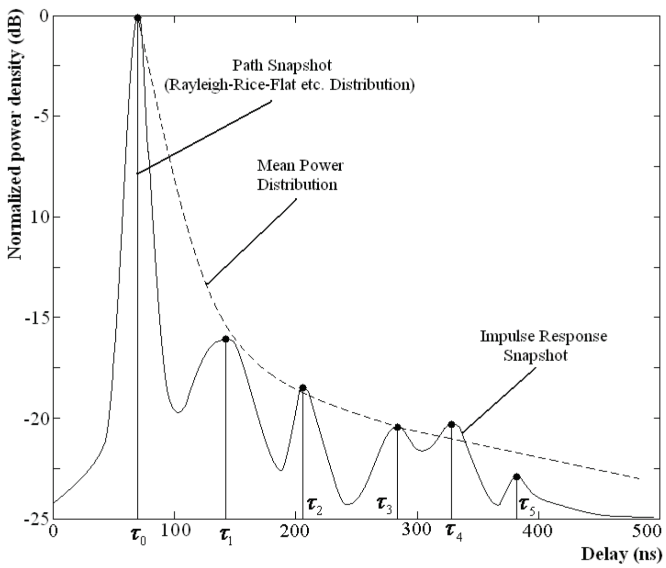

istics are considered to be time-invariant for simplicity and in order to configure a reference platform generally adopted.

The interested reader may refer to the GSM standard model (GSM, 1991), the JTC-PCS standard model (JTC, 1994), the COST207 standard model (COST207, 1986) etc.

Simulation Model of Wideband Channels in the Frequency Domain — Autoregressive Modeling

It is often desirable to simulate frequency selective fading in the frequency domain. The frequency response of the channel may be indirectly calculated via Fourier transformation of the impulse response or directly modeled using autoregressive models. Then, the impulse response of the channel may be indirectly calculated via inverse Fourier transformation.

An autoregressive process would use an all-pole finite filter in order to produce frequency response samples of the radio channel under study. More specifically, for a sample of frequency response measurements, the respective filter poles are calculated and then the statistics of the filter poles are determined. Then, in order to simulate the radio channel, the filter poles are randomly generated using their respective distributions, and the frequency response arises as the output of the generated filter (Pahlavan, 1995).

The frequency response for a specific frequency and time instance will depend on the frequency response at the same time instance and previous frequency values, as shown by

$$T(f_n, t) = \sum_{i=1}^{p} a_i T(f_{n-i}, t) + V(f_n) \tag{12}$$

where $V(f_n)$ is a white noise stochastic process with zero mean value, and a_i are the model's parameters. Using the z-transform operator in equation (12), it comes out that the frequency response $T(f_n,t)$ is the output of a linear filter given by

$$H(z) = \frac{1}{1 - \sum_{i=1}^{p} a_i z^{-1}} = \prod_{i=1}^{p} \frac{1}{(1 - p_i z^{-1})}. \tag{13}$$

Equation (13) corresponds to an all-pole filter. A frequency response sample consisting of, e.g., N frequency points, may be approximated using the p poles of equation (13), while usually it will be that $N > p$. It is noted that each sample generated by equation (12) also includes the impact of the white noise $V(f_n)$, and that the standard deviation of $V(f_n)$ is constant with frequency.

A critical attribute of autoregressive models is the model's order, i.e. the number of poles p. In relative reposts in the literature for indoor environments, the maximum selected order is five (Howard, 1991), but second-order filters are also reported to yield satisfactory results.

Comparison Between Simulation Techniques in Time Delay and Frequency Domain

Simulation in time delay domain is more popular and broadly accepted, mainly due to the fact that there is a one-to-one interpretation between model and natural channel characteristics (time delay and envelope amplitude distribution, Doppler spectrum etc.). Furthermore, all standards committees have developed extensive channel models in the time domain, thus offering a common reference platform.

On the other hand, it is difficult to implement automated algorithms in order to recognize and statistically classify time delays of arrival. Therefore, appropriate techniques must be developed in order to automatically recognize local maxima of the impulse response, the number of incoming paths, the amplitude distributions and time delay of arrival. However, some local maxima may arise due to noise rather than an incoming path.

As long as frequency domain simulation is concerned, there is not a direct interpretation of natural channel characteristics to model parameters. Furthermore, it is a common phenomenon that the impulse response calculated via inverse Fourier transform exhibits more local maxima than the corresponding impulse response which was directly calculated in the time domain. However, the classification and configuration of all-pole filters of autoregressive processes is much easier automated (Pahlavan, 1995).

VII. A STATISTICAL MODELS FADING SIMULATION TOOL

Introduction

A tool for the simulation of small scale fading in mobile channels using statistical models is presented next. The tool has been implemented in MATLAB and offers the ability of evaluating a radio channel's small scale fading characteristics via calculation of mean power, level crossing rate, average fade duration, BER etc (Mitilineos, 2004). It is based on user-defined PDFs for certain channel characteristics in order to evaluate a radio channel with respect to BER performance. For verification purposes, this tool has been applied to a Rayleigh radio channel, for which there exist analytic formulas as well as well-established tools for BER calculation. Then, it was applied to a GBSBEM radio channel for which no analytical formulas or other simulation reports exist. Furthermore, the tool's ability of simulating the case of directional or switched-beam arrays is also presented. The most interesting characteristic of the proposed simulator is the fact that it is based on an open architecture, allowing the implementation of any desired radio channel model.

Channel Simulation

Rayleigh channel simulation is based on vector summing of sinusoidal carriers, according to Figure 1 and equations (4), (5). The resulting received signal envelope is Rayleigh distributed. On the other hand, GBSBEM channel simulation could be implemented by using a tapped filter, like in Figure 3 and 4, but each tap does not suffer from Rayleigh fading. Rather, the AoA distribution for each tap will be biased towards the LOS between transmitter and receiver, and therefore the envelope of each tap is not Rayleigh distributed. For comparison purposes, it is selected herein to simulate a narrowband GBSBEM channel, i.e. a channel with one tap only (flat fading). This implies that it is assumed that $\tau_m - \tau_0 < T_b$, where τ_m is the maximum delay of arrival, corresponding to the boundary ellipse in Figure 5, τ_0 is the delay of arrival corresponding to the LOS, and T_b is the bit period. Incoming components are considered of equal power, while the phase of each incoming component is considered uniformly distributed in $[0,2\pi)$. The AoA of each component will be given by (Liberti, 1999)

$$f_\varphi(\varphi) = \frac{1}{2\pi\beta}\frac{\left(r_m^2 - 1\right)^2}{\left(r_m - \cos\varphi\right)^2}, -\pi \leq \varphi \leq \pi \tag{14}$$

Furthermore, the number of incoming components is selected to be equal to 50. An important detail is that the simulation procedure is executed for a time window, and then the scatterers' positions are re-arranged (i.e. the AoAs and phases of incoming components are re-initialized). As a result the fading signal is not constant during simulation time. Thus, the channel is assumed to be non-static (rather is semi-static), and the 50 simulated components are not constant during simulation. This strengthens the accuracy of simulation results.

In Figure 9, a block diagram of the proposed simulator is illustrated. Initially, a pseudorandom bit sequence is implemented, and then the baseband signal is constructed. Based on whether Rayleigh or GBSBEM channel model is to be simulated, N=50 incoming components are generated, having unitary amplitude and appropriate AoA distribution. The AoA distribution is either uniform or follows equation (14) for a Rayleigh or GBSBEM channel respectively. Thus, a frequency flat fading signal is generated. If the generation of frequency selective fading signals is desired, the same procedure is repeated with appropriately shifted delays as well as different normalized incoming signal amplitudes. Finally, white noise is added (Additive White Gaussian Noise – AWGN), taking into account the selected Signal to Noise Ratio (SNR), and the BER is calculated.

Numerical Results

The equivalent bandpass signal of a BPSK sequence with length equal to 65535 bits is generated, while the transmitting rate is set equal to 100kbps. The signal is 8 times oversampled, and root-Nyquist pulse shaping filters are assumed at both the transmitter and receiver. A fading signal is simulated via 50 uniform-phased incoming components. The Doppler shift of each component is calculated by the AoA and the mobile's velocity. All incoming components are summed and normalized in order that their mean power is unitary. The fading signal is multiplied with the transmitted signal and the fading-distorted signal is constructed. Then, the noise level is calculated via the assumed SNR level. The noise level is calculated in a way that discrete steps of E_b / N_0 values from 0 to 10dBs are simulated, where E_b is the mean bit energy and N_0 is the noise power spectral density. Based on the calculated noise level, AWGN samples are created and added to the fade-distorted signal. The final signal passes through the root-Nyquist receiver filter, and then a sampler and a comparator, where it is compared to a time delayed version of the initial generated sequence. Thus, the number of false received signals and BER are calculated. The procedure is repeated anew with a newly generated symbol sequence, new AoA values and incoming components phases, as well as new noise samples; the procedure is repeated 100 times for each E_b / N_0 ratio value. A maximum Doppler shift equal to v_m = 16Hz, which corresponds to a MS velocity of u = 2m/sec, which is a reasonable velocity for a pedestrian moving in indoor environment, is selected. The MS is assumed to move on the LOS line and draws away from the receiver. A block diagram of the simulated telecommunications system is shown in Figure 10.

The effect of a directional array may also be simulated. As an example, consider a perfect directional array pointing towards the transmitter's direction, with unitary radiation pattern at an angular interval of $\pm 20^o$ around the LOS line and zero elsewhere. Again, we assume 50 incoming components, but now many of them will be rejected by the directional array.

Figure 9. Block diagram of the proposed simulator

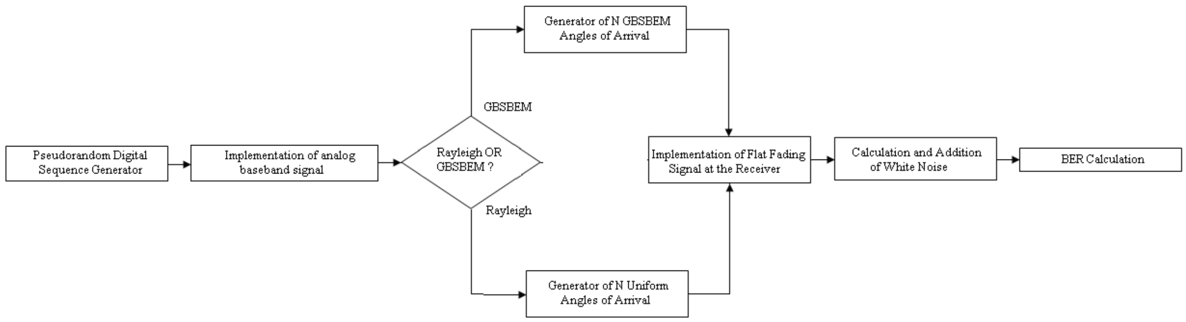

Figure 10. Block diagram of a simple telecommunications system

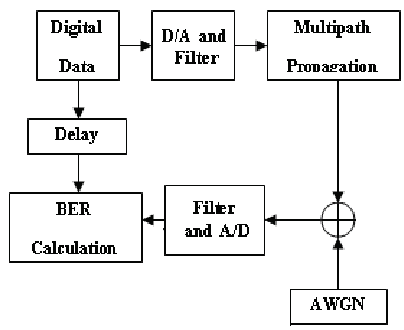

Figure 11. BER plots in the case of a BPSK system with Rayleigh flat fading

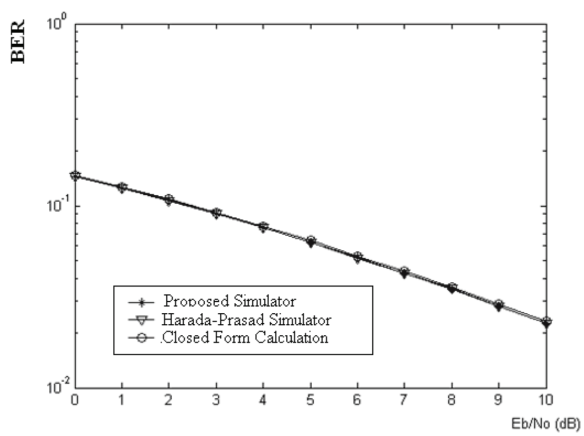

As long as the Rayleigh channel is concerned, there has been implemented a simulator by Harada-Prasad (Harada, 2002), but there is also a closed-form formula for BER calculation as given by

$$BER_{BPSK-FLAT-FADING} = \frac{1}{2}\left(1-\left(\sqrt{1+\frac{1}{E_b / N_o}}\right)^{-1}\right). \tag{15}$$

In Figure 11 the respective numerical results for the proposed and the Harada simulator, as well as the analytic formula of equation (15) are illustrated. The results of the proposed simulator are in excellent agreement with the other two methods, forming an argument for the accuracy of the proposed simulator.

A similar procedure has been followed for the simulation of GBSBEM flat fading. The value of r_m is selected to be equal to 1.585, and arises from equation (2) with an attenuation factor of n = 2, loss factor L_r =6dB, and power threshold T = 10dB. The respective results for an omnidirectional and a directional receiver are illustrated in Figure 12. The directional receiver yields improved BER levels than the omnidirectional one as expected. However, the improvement is not much significant. A possible explanation for this is the fact that, despite the many incoming components discarded by the directional antenna, there are still many components arriving and contributing to flat fading.

Finally, in Figure 13 the more realistic case of a channel with a few incoming components is presented. In this case the Central Limit Theorem cannot be applied and the results of Gaussian PDF for the sum of incoming components are not valid (McPherson, 1990). In the literature, there are research results that handle the problem of the PDF of the sum of limited number of incoming components (Polydorou, 1997; Vellis, 2000). For the specific case, we assume 6 incoming components, which arrive at the receiver with GBSBEM AoA distribution. The maximum normalized delay is set equal to r_m = 1585. An omnidirectional and the perfect directional receiver described earlier are used. Due to the small number of components, the existence of a LOS component is forced to the simulator, i.e. if none of 6 generated components does not arrive from the LOS direction, we add another LOS component arbitrarily. As shown in Figure 13, there is a significant improvement to the resulted BER in the case where a directional receiver is used.

Resume

A simulation tool for the performance evaluation of telecommunications systems with respect to small scale fading is presented. The proposed tool allows for the simulation of any desired user-defined channel model, directional

Figure 12. BER plots in the case of a BPSK system with GBSBEM flat fading, omnidirectional and perfect directional receiver

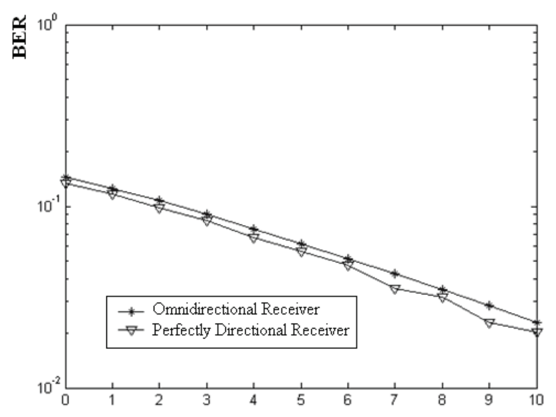

Figure 13. BER plots in the case of a BPSK system with GBSBEM flat fading, Low Multipath, omnidirectional and perfect directional receiver

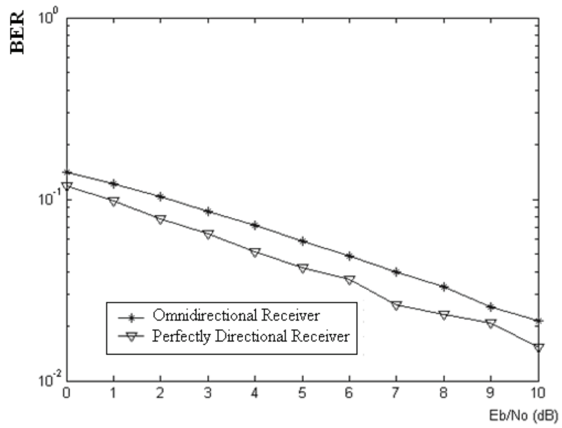

or omnidirectional antenna, E_b / N_0 ratio etc., due to its open architecture. It has been validated via simulation of the classical Rayleigh flat fading channel, and results for a GBSBEM channel are also presented.

VIII. DETERMINISTIC MODELS

Deterministic models calculate the mobile channel impulse response or the signal envelope distribution by using architectural or topographical plans of a specific site. Deterministic models are mainly used in mean attenuation and large scale fading modeling, but are not so broadly used for small scale fading simulation. One reason for this is that the finest possible resolution is needed in order to simulate small scale fading, which results to large or prohibitive computational cost and simulation time. Nevertheless, as the usage of architectural or topographical plans in electronic form is expanded, as well as computational power of modern units is leveraged, deterministic small scale fading modeling is becoming more and more popular.

Another argument that might be raised against deterministic modeling is that the results of deterministic models are valid for the specific site only. However, this is valid for on-site measurements too. Additionally, deterministic simulation of a large number of architectural or topographical plans may yield statistical models too, just like on-site measurements campaigns. On-site measurements are more accurate but also more costly than deterministic channel modeling, and one can choose between the two of them based on his needs and resources.

Deterministic models have been based on geometric optics or ray-tracing techniques. These techniques can be applied to simplified environment models and their execution time is not strongly affected by the dimensions of the environment under study. More complicated ray-tracing techniques include diffraction and scattering phenomena. A major advantage of these techniques is that they can model the AoA of incoming components.

Another approach, which has only recently been proposed due to the large computation cost related, is to solve Maxwell equations for a specific site, taking into account the boundary conditions on the objects and the bounds of the environment. This approach is mainly used for sites of small size. Some techniques used for this purpose are the Finite Differences in Time Domain (FDTD), Method of Moments (MoM), and other.

Ray-Tracing Algorithms

Ray-tracing algorithms simulate channel response using geometric optics techniques. They are simple, while at the same time offer the ability to calculate the power to AoA profile and AoA distribution, and can be applied to indoor as well as outdoor environments (Lebherz, 1989; Lebherz, 1992; Lawton, 1991; Lawton, 1992; Rappaport, 1992; Holt, 1992; Rossi, 1993; Yang, 1993a; Yang, 1993b).

Ray-tracing techniques may incorporate propagation mechanism in free space, as well as propagation via materials – refraction, reflection, diffraction, scattering, diffusion over rough surfaces etc. They may be three-dimensional or two-dimensional. Three-dimensional techniques offer the ability to model channels with antennas placed at different heights or, in the case where the antennas are placed at the same height, they offer the ability to model scatterers at various heights, such as roofs, floors, etc. Generally, they are more accurate but also much more complicated than two-dimensional techniques.

For refraction and reflection, a popular method of analysis is via image theory, where the images of transmitter and receiver are considered on the reflective surfaces, and thus the actual paths of propagation between transmitter and receiver are determined (McKown, 1991; Rustako, 1991). Using this technique, the problem solving procedure may become very computationally intensive, as the number of refractions/reflections taken into account increases. Another ray-tracing approach is the so-called ray-shooting technique (Deschamps, 1972; Ikegami, 1991). With this method, a virtual sphere around the transmitter is separated to solid angle intervals. Each interval corresponds to a ray propagating in space. The propagation is assumed to end in the case where the solid angle's surface reaches the receiver or in the case where the ray power falls below a threshold.

A more specialized and interesting problem is the multiple reflections and refractions within a flat surface with non-negligible thickness, where it can be shown that the multiple reflections and refractions may be modeled with a unique reflection and refraction factor (Burside, 1983). Furthermore, diffraction may arise in the case where the propagating wave is scattered by pins, tips and in general narrow and surfaces of oblique angles. In this case, the diffracted propagating wave is calculated using the Huygens principle and the diffraction coefficient determines the percentage of power which is diffracted towards the receiver. Finally, the phenomenon of diffusion arises in the case where the wave reflects from a rough surface, whose roughness is significant compared to the wavelength. In this case, the wave is not reflected, but rather diffused to all directions. Similarly to diffraction, this case may also be affronted by a point source placed at the point of incidence (Pahlavan, 1995). The diffusion factor is used in order to calculate the percentage of power which is diffused to the direction of the receiver.

In the literature, a number of research papers on ray-tracing algorithms can be found. Catedra et al. have presented a number of ray-tracing techniques, based on micro- and pico-cells applications (Catedra, 1998). Seidel and Rappaport suggested a ray-tracing model for PCS systems inside buildings (Seidel, 1994). Building modelling is performed using AutoCAD, while only large-sized objects with respect to the wavelength are incorporated. Smaller objects are neglected, mainly in order to cut off computational cost, but this poses some limitations on calculating the mean attenuation and large scale fading characteristics. Rizk et al. reported a ray-tracing technique for two-dimensional environments and micro-cells (Rizk, 1997), which is based on reflection and diffraction theory, as well as image theory. Yang et al. presented a ray-tracing technique, based in tetrahedral "ray-tubes" which are used in order to implement their method (Yang, 1998), while the respective application calculates multiple reflections and refractions of the propagated wave. Liang and Bertoni presented a novel ray-tracing technique, which significantly reduces the computational cost for outdoor environments and is based on the assumption that most scatterers in outdoor environments are vertically oriented wall surfaces (Liang, 1998). Fimally, Son and Myung reported a ray-tracing method for quasi-three-dimensional environments (Son, 1999). Their method is based on the "ray-tube tree" structure, while was further extended by Choi et al. in order to incorporate three-dimensional environments, as well as waves penetrating inside buildings (Choi, 2006).

Numerical Solution of Maxwell Equations—FDTD, MoM and UTD Methods

Another approach to deterministic simulation is by directly solving Maxwell equations for a specific environment. Numerical solution of Maxwell equations requires the construction of a grid of points on which differential equations will be numerically solved. The dimensions of the grid must be in the order of wavelength for accurate solution, which means that the computational intensity of the problem increases geometrically with frequency of the site's dimensions. Therefore, this approach demands the availability of extremely large computational power, which until recently was not easily available.

FDTD Method

Due to the evolution of computing systems, field equations solving has matured and attracts the interest of research community. A popular numerical method of Maxwell equations solving is the Finite Differences Time Domain (FDTD) method, where Maxwell equations are approached by finite differences in the time domain. The electric and magnetic field are solved in the time domain, therefore transient response is also calculated. In its first version, the FDTD method was proposed with orthogonal grid (Yee, 1966; Taflove, 1975), but since then it has been improved by utilization of various grid shapes, as well as other techniques for the speed-up of the solving procedure (Holland, 1983; Fusco, 1990; Harms, 1992; Lee, 1993; Yang, 1993a).

Compared to ray-tracing, FDTD techniques are much more demanding in time simulation and computational resources. It is not coincidental that research reports on FDTD channel modeling have been proposed only recently. Talbi presented a FDTD method for UHF wave propagation modeling in indoor environments, while utilizing the reciprocity principle in order to evaluate the effect of directional transmitter and receiver antennas (Talbi, 2001). Wallace and Jensen presented a model which evaluates MIMO systems by simulating wideband signals propagating into simplified two-dimensional indoor channel models (Wallace, 2003). Finally, Papamichael et al. reported the application of a FDTD method in indoor simulation at 434MHz (Papamichael, 2003).

Despite the requirements in computation power, the solution of the electromagnetic problem is much more accurate compared to ray-tracing results, but FDTD channel modeling is not always better than ray-tracing modeling (Pahlavan, 1995). An important reason is that, in fact, the true channel is much more complicated than any electromagnetic model used by FDTD or ray-tracing. Various small objects and details of the channel can never be exactly represented in a three-dimensional channel representation, and therefore the real channel is always different than the model. Therefore, ray-tracing as well as FDTD or other electromagnetic methods have an upper limit of accuracy. Nevertheless, as the channel representation model becomes more accurate, FDTD method will yield more accurate results than ray-tracing methods.

Hybrid UTD-MoM Method

Uniform Theory of Diffraction (UTD) techniques have been also proposed for channel modeling. This type of techniques is classified between ray-tracing and FDTD techniques with respect to computational power requirements. Zhang presented a simulation model based on UTD for wideband cellular systems (Zhang, 1997). Zhang's model is able of calculating mean attenuation values using UTD models, using a narrowband transfer function calculated by UTD, which takes into account refracted as well as reflected waves. O'Brien et al. presented an application where the UTD method is used together with analytic propagation formulas in order to model three-dimensional, indoor as well as outdoor environments (O'Brien, 2000). Finally, Oestges et al. presented a model based on a combined UTD and ray-tracing method (Oestges, 2002).

Recently, the possibility of using a hybrid MoM-UTD method for channel modeling has been presented in (Mitilineos, 2005; Varlamos, 2006). The UTD method is used alternatively to ray-tracing in order to model wave propagation and interaction with various dielectric materials, while the MoM method is used alternatively to FDTD in order to take into account the effect of metal and conductive surfaces (e.g. antennas and other surfaces). This hybrid method is classified as deterministic modeling, and more specifically as a electromagnetic field equations solving technique.

Comparison Between Statistical and Deterministic Models

Statistical models demand the minimum computational power among other model types but, in general, due to the fact that they are based on geometric assumptions of the natural channel characteristics, the corresponding simulation results are of least accuracy and are generally used as reference platforms for comparison purposes. The same is valid for statistical models that arise after measurements campaigns too. However, an advantage of these models is that they can be used as a good starting estimation.

Measurements based models are the most accurate and arise after measurements in a specific site but are valid for the specific site only. These models demand the least computational power, but have the disadvantage that for each specific site, a new set of measurements is required; a procedure which is time and money consuming, and sometimes not even applicable.

Finally, deterministic models demand the most computational power, and are more accurate than statistical and less accurate than measurements based models. Deterministic models, just like measurements campaigns, may be used in order to extract a statistical model. An advantage of deterministic models with respect to statistical models is that they are more applicable for selecting specific transmitter and receiver positions in a site.

Within the deterministic models class, ray-tracing techniques are characterized by strongly increasing complexity with the complexity of the environment model used. This means that it is not the size of the environment but the detail depth of the analysis, e.g. number of reflections, refractions etc. that are taken into account, the detail in objects and surfaces representation etc. On the contrary, FDTD techniques complexity increases strongly with an increase of the environment size or frequency, just like the hybrid MoM-UTD method.

IX. RESEARCH RESULTS—A SIMULATION TOOL FOR DETERMINISTIC MODELING OF INDOOR ENVIRONMENT

Introduction

A deterministic simulation tool for indoor mobile channel environments has been developed and presented in (Mitilineos, 2005). It is based on the hybrid MoM-UTD method and the SuperNEC application (Fourie, 2000), while it has been validated using indoor environments measurements results in the literature.

As aforementioned, small scale fading characterization is mainly implemented using statistical/geometric models, especially during early design stages. However, during final design stages, the initial assumptions need to be validated using on-site measurements, like in (Alexander 1982; Saleh, 1987; Rappaport, 1989; Hashemi, 1994; Kim, 1996) and other. Unfortunately, on-site measurements are extremely time and money consuming, or even non-applicable some times. Deterministic modeling is proposed to cover the gap between inexpensive, simple but low accuracy statistical models and expensive, resource draining, but high accuracy on-site measurements. It is a good choice only in the case where there is enough computational power available, and is mainly used in indoor environments.

The technique used herein is based on a hybrid MoM-UTD method. Simplified model of the site under simulation are used, while transmitter and receiver antennas are placed therein according to user requirements. Then, the frequency response is calculated, which is used in order to calculate the channel impulse response via Inverse Fast Fourier Transform (IFFT). The simulation procedure can be repeated for various neighbouring receiver positions, thus simulating receiver's moving. Having in hand the frequency and impulse response of the channel for multiple receiver positions, we are able to obtain information regarding its statistical characteristics, such as rms delay spread. As will follow, the numerical results obtained using our model are in excellent agreement to relative measurements in real environments (based on reports by Hashemi and Tholl (Hashemi, 1994) and Kim et al. (Kim, 1996)).

Model and Tool Description

Electromagnetic Model

The proposed deterministic simulation tool is able of offering accurate results regarding wave propagation using simplified representations of the propagating environment, in LOS as well as NLOS cases. A typical indoor environment shall include a floor and a roof, walls, furniture, office machinery, people etc., as well as a number of transmitting and receiving antennas.

The propagation environment model is created using SuperNEC, which incorporates the hybrid MoM-UTD method. UTD primitives (UTD is used for dielectric surfaces modeling) are two-dimensional rectangular surfaces with a desired thickness, as well as dielectric cylindrical surfaces. Typically, three reflections over dielectric materials and one reflection over conductive materials, one refraction and one combination of either refraction-reflection or reflection-refraction are taken into account; however the number of reflections and refractions taken into account may change according to user's requirements. The UTD method incorporated in SuperNEC yields credible results in the case where the dielectric surfaces are much larger compared to the wavelength. On the other hand, MoM segments are conductive, straight metallic pieces, with a cylindrical shape and a user-specifiable length (Fourie, 2000).

Roofs, floors, doors, walls and in general all dielectric materials are simulated by UTD, while antennas, reflectors, and in general all metallic materials are simulated by MoM. The necessary input data for dielectric materials include the dielectric permittivity ε_r**,** the magnetic permeability μ_r, the conductance *sigma* and the material's thickness, length and width. Naturally, all these parameters will correspond to actual measurements of real materials. On the other hand, for conductive materials the necessary input data include the conductance, the thickness, length and width, as well as the segment density per cm^2**.**

Mathematical Description of the Proposed Method

As mentioned before, the proposed application is based on the calculation of the channel's frequency response. The transmitting antenna is excited by sinusoidal carriers of unitary amplitude and zero phase. The antenna is excited over a large frequency range with constant frequency step. Let the frequency range be *B*, the frequency step be f_s; then *N* carriers are transmitted in total, where

$$N = B/f_s + 1. \tag{16}$$

The width and phase of the signal at the receiving antenna output are obtained by SuperNEC for each frequency tone, and thus the frequency response of the channel is recorded. Then, the channel's impulse response is calculated via IFFT. The resolution of the impulse response at the time delay dimension (delay step) is given by

$$\tau_{step} = 1/B \tag{17}$$

while the impulse response has a period which is given by

$$T = 1/f_s. \tag{18}$$

The detected incoming components are identified by the local maxima of the impulse response. A relative power threshold is specified, below which no local maxima are taken into account. The equivalent complex bandpass representation of the impulse response is given by,

$$h(t) = \sum_{i=1}^{L} \beta_i e^{j\varphi_i} \delta(t - \tau_i) \tag{19}$$

where *L* is the number of incoming components and β_i, ϕ_i, τ_i are the amplitude, phase and delay of the *i*-th component respectively (Pahlavan, 1995).

Setup Description for a Simplified Indoor Environment.

A simplified indoor office and NLOS environment is displayed in Figure 14, where propagation in the band 2.4-2.5GHz is studied. The room dimensions are 16m × 10m × 4m, while the brick wall in the middle of the room has a height of *h* = 4m and a width of *l* = 8m. The electrical characteristics of the inner and outer walls at the center frequency (*f* = 2450 MHz) are set to $\varepsilon_r = 4.5$, *sigma* = 0.027 s/m and $\mu_r = 1$ while for the roof and floor they are $\varepsilon_r = 8$, *sigma* = 0.095 s/m and $\mu_r = 1$, and are all selected in order to correspond to actual measurements of real materials (Yang, 1998). The walls thickness is set equal to 0.115m, while the roof and floor thickness are set equal to 0.1m.

Furthermore, the transmitting (TX) and receiving (RX) antennas are identical, vertically polarized dipoles. Their centers are placed at a height of 1.5m, while their length and radius are equal to 0.0555m and 0.001m respectively, thus resonating at 2.4GHz. The terminating (load) resistance at the receiver is set equal to 75Ω.

The channel behavior, as long as small scale fading is concerned, is recorded by measuring the frequency response for various receiver positions. The bandwidth is set equal to B = 100MXz, with upper and lower frequencies equal to f_1 = 2400 MHz and f_2 = 2500 MHz respectively. The frequency step is set equal to f_S = 100 kHz; thus for each receiver position we collect N =1001 measurements of the voltage at the receiver's output. The receiver is assumed to move towards the transmitter with a low constant velocity of lm/sec, and covers a distance of lm orm 8.2λ, λ being the wavelength. The initial transmitter-receiver separation distance is equal to 9m, while the frequency response is collected every 2cm. This means that by the end of the procedure, there are 51 channel frequency responses available. Thus, via IFFT, we take 51 impulse responses, with step and period at the delay dimension equal to $\tau_{step} = 1/B = 10\text{ns}$ and $T = 1/f_s = 10\mu\text{s}$ respectively.

Numerical Results

Some channel impulse responses are presented in Figure 15. The frequency response of Figure 15b corresponds to a receiver position placed λ / 6 apart from the receiver position which corresponds to Figure 15a, while in Figure 15c the receiver is placed 2λ apart from Figure 15a. As can be seen in Figure 15c, there is an incoming component with delay 50ns, which is not visible in the other Figures. Furthermore, in Figure 5.15d the "average" impulse response, $h_{avg}(t)$, is displayed. The average impulse response is calculated by summing the impulse response at each receiver position and then dividing with the total number of positions, and reflects average channel behaviour.

Indicatively we mention that, on the average, we needed 1.84sec in order to calculate the frequency response at each receiver position and frequency tone. The overall simulation time may be calculated by multiplying 1.84sec times the number of frequency tones and receiver positions. Furthermore, in order to evaluate the simulation time in other environments, we modeled and simulated the building described in Kim et al. (Kim, 1996), where we needed on the average 3.89sec for each receiver position and frequency tone. All simulations are executed on a standard Pentium IV 2.4GHz PC, with 512MB of RAM.

The effect of multipath fading and the level of Intersymbol Interference (ISI) are determined by the rms delay spread, which is given by,

$$\tau_{rms} = \sqrt{\mathrm{E}(\tau^2) - \left(\mathrm{E}(\tau)\right)^2} \tag{20}$$

where

$$\mathrm{E}(\tau^n) = \frac{\sum_{i=1}^{L} \tau_i^n \beta_i^2}{\sum_{i=1}^{L} \beta_i^2} \tag{21}$$

while β_i, τ_i are the amplitude and delay of the i-th component respectively (Pahlavan, 1995).

For each receiver's position, the rms delay spread of the impulse response, $\tau_{rms,i}$, is calculated, and then the average and standard deviation of the rms delay spread, μ and respectively, are calculated using,

$$\mu = \frac{\sum_{i=1}^{N_s} \tau_{rms,i}}{N_s} \tag{22}$$

$$\sigma = \sqrt{\frac{1}{N_s - 1} \sum_{i=1}^{N_s} \left(\tau_{rms,i} - \mu\right)^2} \tag{23}$$

where $N_s = 51$ is the number of different receiver positions. The relative results are included in Table 1, together with respective results taken by measurements in two building types (A and B) which are included in (Hashemi, 1994). There are two threshold power values, below of which the multipath components are neglected. In the first case, $T_{threshold,1} = 20$dB, the average is equal to $\mu_1 = 15.53$ns and the standard deviation equal to $\sigma_1 = 3.78$ns, while in the second case, $T_{threshold,2} = 30$dB, the respective values are $\mu_2 = 17.70$ns and $\sigma_2 = 4.80$ns. The mean spread is larger in the second case, since more components take part into the calculation of the delay spread, and usually lower power components arise for longer time delays. All results are in good agreement with (Hashemi, 1994).

The "average" impulse response, $h_{avg}(t)$, offers an alternative means of channel characterization. For the two examined cases, $T_{threshold,1} = 20$dB $T_{threshold,2} = 30$dB, the average impulse responses are extracted and the rms delay spreads are calculated. In the first case, the result was $\tau_{rms,1}(h_{avg,1}) = 15.42$ns, while in the second case the result was $\tau_{rms,2}(h_{avg,2}) = 16.79$ns. Both these values are in good agreement with the average rms delay spread values given in Table 1.

Furthermore, the statistical behavior of the channel is examined deeper, by calculating the PDF of the rms delay spread. For this cause, Mean Square Error (MSE) tests are performed for all $N_s = 51$ impulse responses $\tau_{rms,i}$ which were collected during receiver movement. Then, MSE was calculated between the empirical distribution arising by simulation and three popular theoretical distributions. More specifically, Rayleigh, Normal (Gaussian) and Weibull distributions are examined. These distributions are given by,

$$f_{X,Rayleigh}(x) = \frac{x}{b_R^2}\exp\left(-\frac{x^2}{2b_R^2}\right) \tag{24}$$

$$f_{X,Normal}(x) = \frac{1}{\sigma_N\sqrt{2\pi}}\exp\left(-\frac{(x-\mu_N)^2}{2\sigma_N^2}\right) \tag{25}$$

$$f_{X,Weibull}(x) = a_W b_W x^{b_W-1}\exp\left(-a_W x^{b_W}\right) \tag{26}$$

respectively, where b_R, μ_N, σ_N, a_W, b_W are appropriate parameters for each distribution.

The MSE is calculated using

$$\text{MSE} = \frac{\sum_{i=1}^{N_{\text{int}}}\left(p_{D,j} - F_j\right)^2}{N_{\text{int}}} \tag{27}$$

where F_j is the empirical Cumulative Distribution Function (CDF), which is given by

$$F_j = \text{prob}\left(\tau_{rms} < \tau_j\right),\ j = 1,\ldots,N_{\text{int}} \tag{28}$$

Table 1. Average and standard deviation of rms delay spread for the setup of Figure 14

Simulation Results				**Building A (B) (Hashemi, 1994)**		**Building A (B) (Hashemi, 1994)**	
$T_{threshold,1}$=20dB		$T_{threshold,2}$=30dB		$T_{threshold,1}$=20dB		$T_{threshold,2}$=30dB	
μ_1 (ns)	σ_1 (ns)	μ_2 (ns)	σ_2 (ns)	μ_1 (ns)	σ_1 (ns)	μ_2 (ns)	σ_2 (ns)
15.53	3.78	17.70	4.80	17.9 (18.4)	4.6 (4.8)	20.8 (20.7)	4.1 (4.4)

Figure 14. Representation of a simplified indoor environment

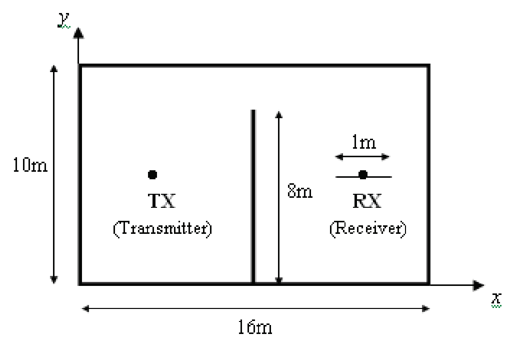

while $p_{D,j}$ is the the theoretical CDF which is given by

$$p_{D,j} = \int_{0}^{\tau_j} f_{X,D}(x)dx \tag{29}$$

where the index D corresponds to the appropriate distribution (R for Rayleigh, N for Normal, W for Weibull). The parameter N_{int} corresponds to a desired number of calculation intervals between the minimum and maximum calculated τ_{rms}, while τ_j is the upper limit for each of the selected intervals. In the following, N_{int} is set equal to $N_{\text{int}} = 25$.

The theoretical PDF corresponding to the minimum MSE is selected. For each distribution, its parameters are calculated using the method of moments (not the electromagnetic MoM). More specifically, the first and second moment of the theoretical distributions are calculated as a function of its parameters, and then set equal to the corresponding parameters of the empirical distribution. The theoretical PDF parameters arise after solving the arising equations.

MSE tests results values for each distribution for both cases, $T_{threshold,1} = 20\text{dB}$ and $T_{threshold,2} = 30\text{dB}$ are tabulated in Table 2. It is concluded that the normal distribution is optimum and followed by Weibull and Rayleigh.

Finally, a comparison among the empirical and theoretical distributions is illustrated in Figures 16 and 17, for the assumed threshold values. It is worth to be noted that similar results regarding the normal distribution as optimally approximating empirical distributions of τ_{rms} are also reported in (Hashemi, 1994).

Resume

Using the proposed deterministic simulation tool, it is possible to extract valid results about the statistical behavior of a radio channel, without having to proceed to on-site measurements. The possibility of calculating statistical characteristics, such as the rms delay spread, but also characteristics such as frequency and impulse response, mean channel response and other are presented. It is worth noted that all results are in good agreement

Table 2. MSE tests results for Rayleigh, Normal and Weibull distributions

Theoretical Distribution of τ_{rms}	$T_{threshold}$=20dB	$T_{threshold}$=30dB
	MSE ($\times 10^{-3}$)	**MSE ($\times 10^{-3}$)**
Rayleigh	35.188	17.535
Normal	**0.438**	**0.664**
Weibull	1.060	0.978

Figure 15. Channel impulse responses for the setup of Figure 14 and various receiver positions

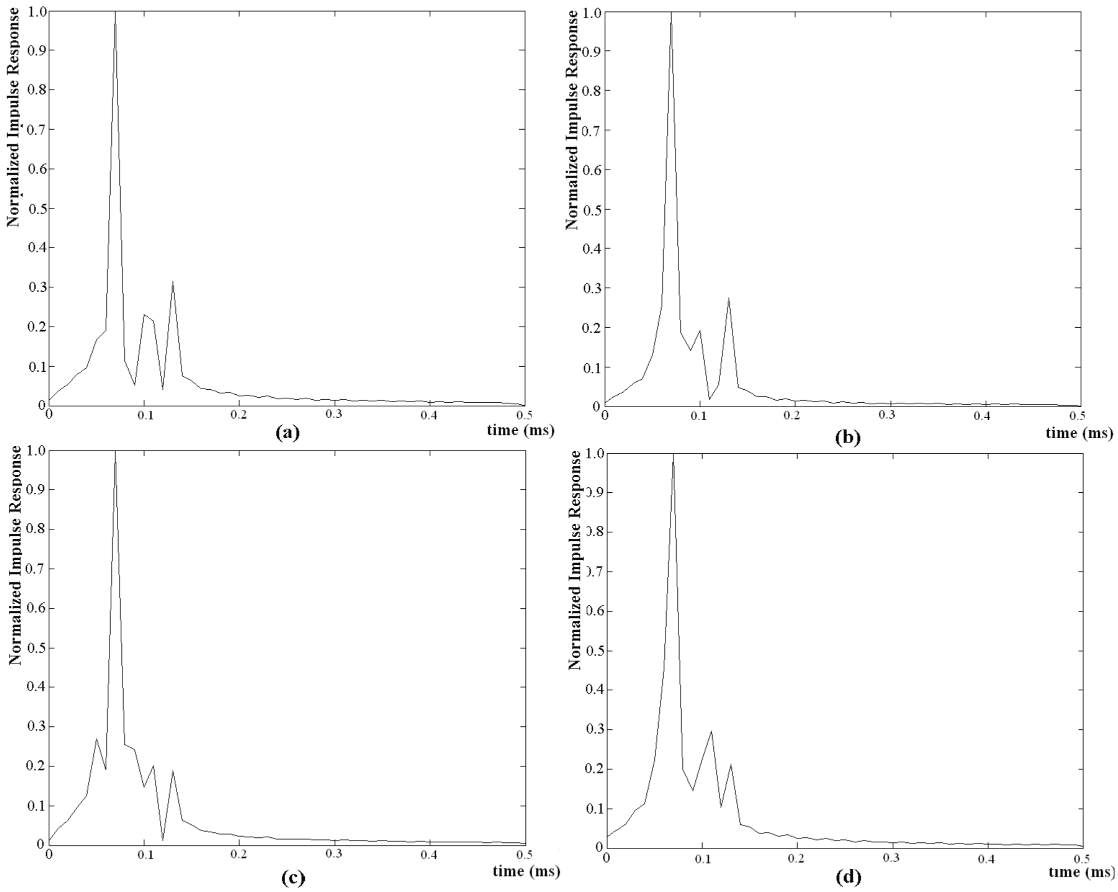

Figure 16. Comparison between empirical and theoretical distributions ($T_{threshold}$=20dB)

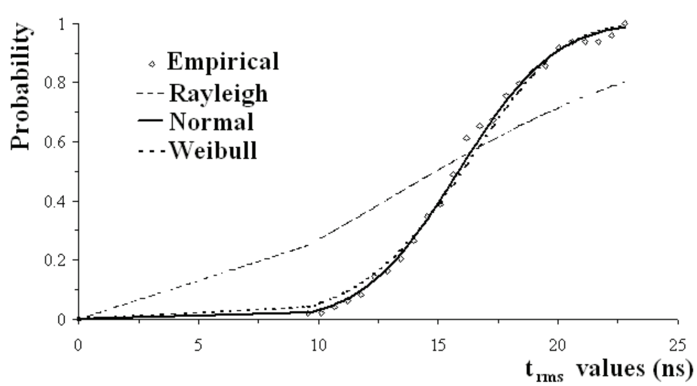

with corresponding measurements results to similar environments. As long as simulation time is concerned, it is not prohibitory, especially if the required spatial resolution is concerned, due to the fact that small scale fading study is required.

It is noted that with the proposed method, it is considered that wideband channel simulation is performed (frequency selective fading), while in the next section the case of narrowband channel simulation (frequency flat fading) is presented.

X. EXTENSION AND APPLICATION OF THE PROPOSED DETERMINISTIC SIMULATION TOOL

Introduction

Apart from drawing conclusions on the statistical attributes of fading in an indoor mobile channel, the proposed deterministic model can be used in a way to include smart antennas evaluation, as well as calculating BER (Varlamos, 2006). The case of use of Switched Parasitic Arrays (SPAs) is herein presented and comparative conclusions are drawn towards the improvement of the link in relation to the use of simple omnidirectional antennas, with respect to both mitigation of multipath fading and BER improvement. The proposed tool has been also used in order to evaluate a novel horizontally polarized switched-beam antenna in [Mit2006a], but this case will not be presented herein.

Rotation of a SPA's radiation pattern is achieved by entering the appropriate digital "word" to the control circuit, through high frequency switches. The ones, "1", of the digital word correspond to loaded elements while the zeros, "0", to short-circuited ones. All active elements are fed with voltage coefficients of equal amplitude and phase, but the amplitudes and phases of the corresponding currents, both in active and parasitic elements, are affected by electromagnetic coupling among all elements. SPAs have been extensively used to switched-beam applications (Preston, 1998; Schlub, 2000; Varlamos, 2003). Herein, the SPAs under examination are characterized by circular symmetry (Tillman, 1966; Sibille, 1997), while their behavior is studied from both the points of "smartness" evaluation as well as directivity alone.

Setup Description

The simulation setup is similar to the one described in Figure 14, but with a few important differences. The environment under study is pictured in Figure 18. The outer dimensions are again 16m x 10m x 4m while the inner wall is 4m high and 8m long. The operational frequency is chosen to be equal to f = 1800MHz. The roof,

Figure 17. Comparison between empirical and theoretical distributions ($T_{threshold}$=30dB)

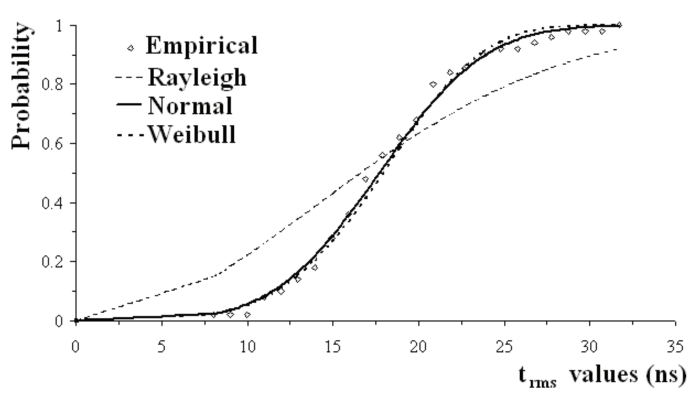

Table 3. Technical and performance characteristics of the SPCA antenna that was used during simulation

Dipoles' Length (λ)	Circle Radius (λ)	Dipoles' Radius (λ)	Gain (dBi)	RSLL (dB)	$\Delta\varphi_{3dB}$ (°)	Z_{in} (Ω)
0.486	0.534	0.001	7.59	-6.45	57.22	91.64+1.01*j*

Figure 18. Representation of the channel and antennas for SPA simulation. A magnified representation of the SPA receiver has been used for clarity purposes.

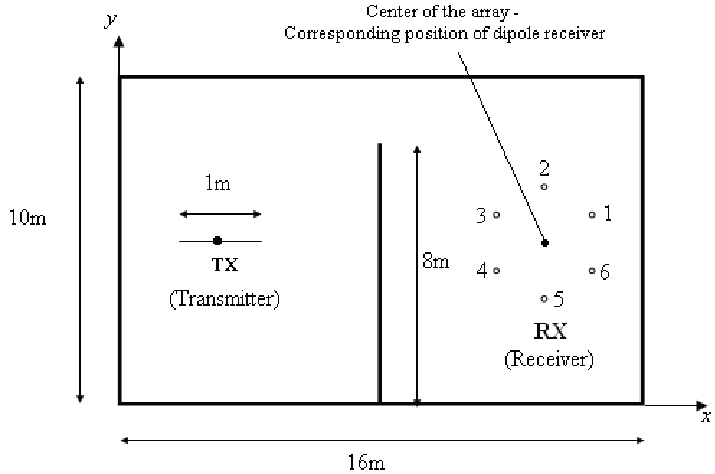

the floor and the inner/outer walls are simulated as UTD elements, with electric attributes for the walls $\varepsilon_r = 6$, $\sigma = 0.02$s/m and $\mu_r = 1$, while for the roof and the floor $\varepsilon_r = 8$ $\sigma = 0.09$s/m, and $\mu_r = 1$ (Yang, 1998).
The antennas of the receiver and transmitter are vertically polarized and placed to 1.5m height. The transmission antenna is a dipole 0.46λ length and range 0.006λ, where λ the wavelength. The receiver antenna is either an identical dipole, when there is no simulation of the smart antenna, or a Switched Parasitic Circular Array (SPCA) when the use of the directional or switched beam array smart antenna is simulated.

The SPCA used has been proposed by Varlamos et al. (Varlamos, 2003). It consists of six vertically polarized identical dipoles, forming a uniform circular layout. The angle of the n-th dipole is $\varphi_n = (2n-1)\pi/6$, where n = 1,...,6.

The SPCA architecture is shown in Figure 18, where it is magnified for clarity purposes. By feeding the n-th dipole and short-circuiting the rest, the antenna is radiating towards the angle ϕ_n. The attributes of the SPCA are tabulated in Table 3. The termination resistance of the receiver is chosen in a way to maximize the power delivered to the load. Consequently in the case where the dipole is used as a receiver the termination resistance is 75Ω, while in the case where the SPA is used the termination resistance is 90Ω.

As a case study, consider transmitting a BPSK signal of power equal to 8.5dBm. A root-Nyquist filter is used at both the transmitter and receiver. A good approximation of the bandwidth necessary to transmit a BPSK signal is given by,

$$B_s = \frac{1.5}{T_b} = 1.5R \tag{30}$$

where B_s is the bandwidth, T_b is the bit period, and R is the transmission rate. The environment of Figure 18 corresponds to an environment of the F-H type, according to the Pahlavan-Levesque guidelines (Pahlavan, 1995), and thus the maximum rms delay spread $\tau_{rms,\max}$, is 0.1usec. Consequently, if a correlation factor of $\rho \geq 0.5$ is selected, then the coherence bandwidth is given by [Rap1999],

$$B_c(\rho \geq 0.5) = \frac{1}{5\tau_{rms}} = 2\text{MHz} \tag{31}$$

For simulation purposes, it is considered that R=0.5Mbps, with carrier frequency 1800MHz, so$B_s = 1.5R$ = 0.75MHz < B_c. The important conclusion from this analysis is that the signal suffers from frequency flat fading. As it was mentioned in Section IX, it is herein attempted to simulate a narrowband signal with frequency flat fading, while it has already been proven the possibility of simulating wideband signals suffering from frequency selective fading.

Simulation Procedure

The transmitter is assumed to move along a straight section of 1m length while the receiver remains fixed. Every 2cm of the transmitter's displacement, measurements of the receiver's output take place at the frequency of f = 1800; totally, 51 measurements for different transmitter positions are collected.

If the receiver is desired to be the SPCA, the output of that radiation pattern providing the maximum power is recorded. Herein, the switching time is considered to be negligible, thus only the maximum power pattern is considered to be active. If the receiver is desired to be a directional antenna, the SPCA is again used, but only one pattern remains active as the transmitter moves. Finally, if the receiver is desired to be an omnidirectional antenna, a dipole identical to the transmitter is used.

BER Calculation

Considering the primary conclusion that the transmitted signal suffers from frequency flat fading, the BER calculation process can be analyzed as follows:

a. For each one of the transmitter's positions, i_p (i_p = 1,...,N_p) – obviously N_p 51-, the received power is calculated according to the formula

$$p_{r,i_p} = \left(|I_c| / \sqrt{2}\right)^2 R_L \tag{32}$$

where $|I_c|$ is the current amplitude induced to the central segment of the active receiver element, and R_L is the receiver termination resistance.

b. The mean value of the received power is calculated using the formula

$$\overline{p_r} = \left(1/N_p\right) \sum_{i_p=1}^{N_p} p_{r,i_p} \tag{33}$$

c. The appropriate mean noise power, σ_n^2, is calculated, so that the BER is calculated for the desired E_b / N_0, using the formula,

$$E_b / N_0 = \overline{p_r} / \sigma_n^2 \Rightarrow \sigma_n^2 = \frac{\overline{p_r}}{\left(E_b / N_0\right)} \tag{34}$$

By using the formula (34), the noise power is calculated for each E_b / N_0 value, which is considered to be constant during the movement of the transmitter.

d. For each position of the transmitter the BER is calculated using,

$$\mathrm{BER}_{i_p} = Q\left(\frac{p_{r,i_p}}{\sigma_n^2}\right) \tag{35}$$

where the equation $Q(.)$ depends on the modulation technique. For the specific case and based to the preceding analysis,

$$\mathrm{BER}_{i_p} = \frac{1}{2}\mathrm{erfc}\left(\sqrt{\frac{p_{r,i_p}}{\sigma_n^2}}\right). \tag{36}$$

e. The mean BER is calculated using

$$\overline{\mathrm{BER}} = \left(1/N_p\right)\sum_{i_p=1}^{N_p}\mathrm{BER}_{i_p}. \tag{37}$$

Besides the proposed method, BER was also calculated using a Monte Carlo technique, where the power measurements to the output were used to develop the fading signal. The results were identical in both cases; therefore the proposed technique provides accurate calculations of BER without the large amount of resources needed for Monte Carlo simulation.

Numerical Simulation Results

For comparison purposes, simulations are conducted for the SPCA performing as SPA as well as a simple directional antenna. Furthermore, three different dipole receiver positions are also examined. The six directional patterns of the SPCA arise by appropriately selecting the element to be fed, while the three dipole positions are at the center of the SPCA, at the 3-rd SPCA element position, and at the 5-th SPCA element position. The mean BER was calculated for E_b / N_0 values from 0 to 12dB, with a step of 1dB.

Simulation results are illustrated in Table 4, where FD is used in order to denote Fade Depth, i.e. the maximum to minimum received power ratio. Furthermore, results for the mean received power as well as mean BER are presented for the case where E_b / N_0 = 10dB.

Table 4. Simulation results of SPA, directional and omnidirectional antennas

Receiver Type, RX	*FD* (dB)	Mean Received Power (dBm)	BER ($\times 10^{-2}$) (E_b/N_0=10dB)
SPCA - switched beam	6.84	-41.61	0.015
SPCA –Element 1 Active	32.40	-50.48	2.974
SPCA –Element 2 Active	11.75	-44.72	0.275
SPCA –Element 3 Active	16.84	-42.30	0.699
SPCA –Element 4 Active	22.28	-44.37	1.716
SPCA –Element 5 Active	9.55	-44.09	0.076
SPCA –Element 6 Active	26.92	-49.84	2.091
Dipole – SPCA Center	13.70	-42.78	0.354
Dipole – Position of SPCA 3rd Element	30.55	-46.18	1.435
Dipole – Position of SPCA 5th Element	19.65	-44.98	0.882

Figure 19. Comparison of received SPCA power to the directional SPCA having it 5th element active

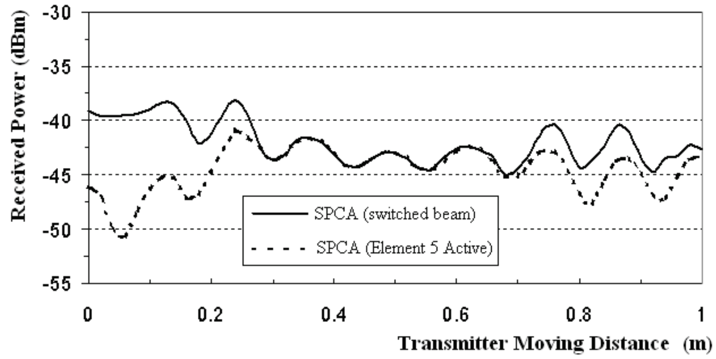

Figure 20. Comparison of the mean BER –SPCA, SPCA directional antenna having its 3rd element active, and SPCA directional antenna having its 5th element active

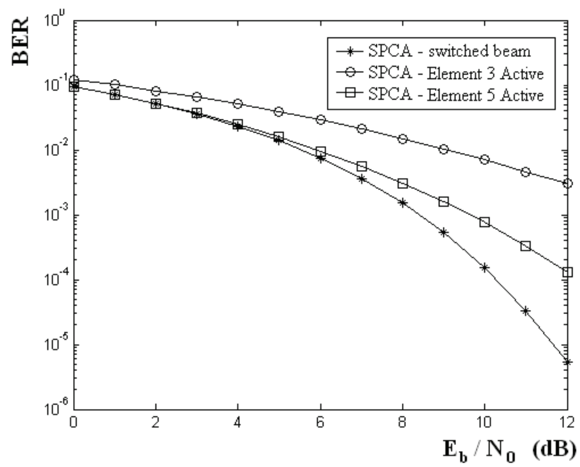

Figure 21. Comparison of received power of SPCA and the dipole placed at the center of the SPCA

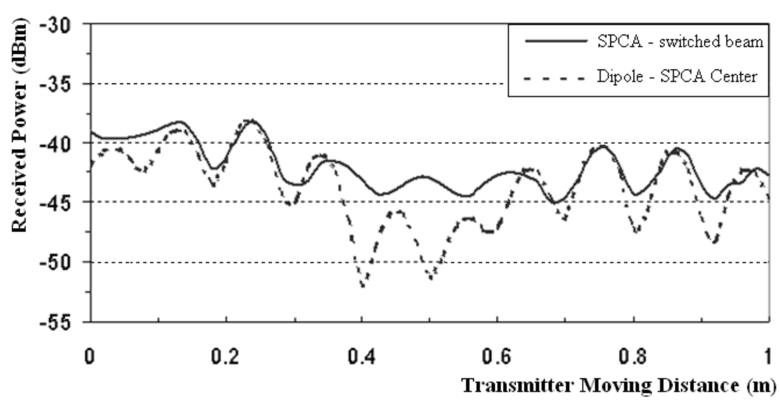

Figure 22. Comparison of the mean BER-SPCA, dipole at the center of the SPCA, dipole at the position of the 3rd element of SPCA, dipole at the position of the 5th element of the SPCA.

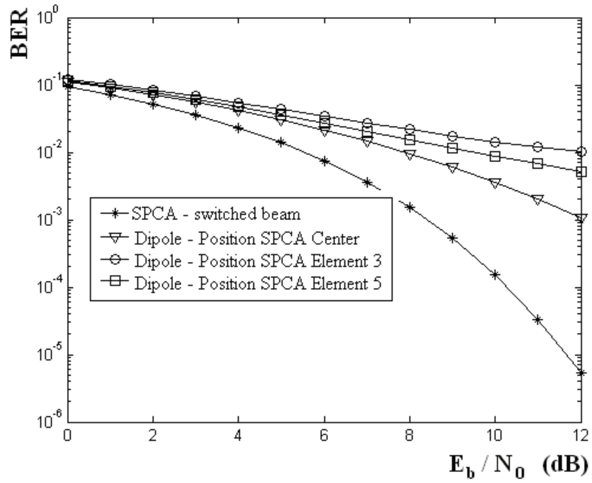

In Figure 19, the received power is depicted with respect to the position of the transmitter when the SPCA and the directional antenna with the 5th element active are used. In Figure 20 the BER plots for the SPA and the directional antennas with the 3rd or the 5th element active are depicted.

Similarly, in Figure 21 the compared received power is presented in the case where the SPCA or the omnidirectional dipole placed at the center of the SPA are used, while in Figure 22 the BER of the SPCA compared to three cases of different receiver positions is illustrated.

Evaluation of Results

From Table 4 and Figures 19-22, it is evident that the SPCA antenna exhibits superior performance in comparison to any other case of directional or omnidirectional antenna, with respect to the fade depth *FD*, the mean received power and the mean BER.

Furthermore, the directional antenna with the 3rd element active presents the maximum received power, as it is directed to the main arrival angle of the receiving signal, while the one with the 5th element active presents the minimum *FD*. Those two directional antennas exhibit enhanced performance compared to the respective cases of a dipole positioned at the positions of the corresponding active elements.

On the other hand, among directional antennas, the worst performance is exhibited by the antennas with their 1st or 6th element active. Maybe this is due to their orientation, since they aim to an angle opposite to that of the transmitter.

Returning to the SPCA, for BER = 10^{-4}, the cut to the transmitted power that can be achieved through its use is 2.25dB and 4.65dB, with respect to the use of the optimum directional or the optimum omnidirectional receiver respectively, as becomes evident from Figures 20 and 22. Finally, it is worth noting that the performance of the SPCA in Figures 19-22 is compared to the cases that the directional and omnidirectional receivers present the least favorable to the SPCA results. The improvement of the performance, in relation to the mean received power, the *FD* and the BER is more impressive if compared to other cases.

As a result, the proposed model has undertaken the necessary adjustments so that it is immediately employable for use in order to evaluate directional and switched-beam antennas, while it is evident that it is possible to simulate both frequency flat and selective fading.

XI. CONCLUSION

The de facto wireless nature of NGNs mandates the development of efficient radio channel simulation techniques in order to rapidly and cost-effectively design and develop NGWNs. Being motivated by this main conclusion, this chapter is focused on small scale fading and aims to present the most popular small scale fading modeling and simulation techniques for the mobile radio channel. Some popular simulation models are presented and classified, while a short discussion took place for each type of technique. Furthermore, two channel simulation tools (one statistical and one deterministic) are proposed and results are presented.

The authors hope that the information provided herein will help researchers to acquire an insight to small-scale fading simulation techniques, and will create a motivation in order to further study this exciting research field.

REFERENCES

Akan, O.B. (2004). *Advanced transport protocols for next generation heterogeneous wireless network architecture*. Unpublished Master thesis, Georgia Institute of Technology, Georgia, USA.

Alexander, S.E. (1982). Radio propagation within buildings at 900MHz, *IEE Electronics Letters*, Vol. 18, pp. 913-914.

Bithas, P., Mathiopoulos, T., and Kotsopoulos, S.A. (2007). Diversity Reception over Generalized-K (KG) Fading Channels, *IEEE Transactions on Wireless Communications*, to be published.

Burside, W.D., and Burgener, K.W. (1983). High frequency scattering of thin lossless dielectric slab, *IEEE Transactions on Antennas and Propagation*, Vol. AP-31, pp. 104-110.

Catedra, M.F., Perez, J., DeAbana, S.F., Gutierez, O. (1998). Efficient Ray-Tracing Techniques for Three-Dimensional Analyses of Propagation in Mobile Communications: Application to Picocell and Microcell Scenarios, *IEEE Antennas and Propagation Magazine*, Vol. 40, No. 22, pp. 437-440.

Chengshan, X., Zheng, Y.R., and Beaulieu, N.C. (2002). Second-order statistical properties of the WSS Jakes' fading channel simulator, *IEEE Transactions on Communications*, Vol. 50, No. 6, pp. 888-891.

Choi, M.S., Park, H.K., Heo, Y.H., Oh, S.H., and Myung, N.H. (2006). A 3-D propagation model considering building transmission loss for indoor wireless communications, *ETRI Journal*, Vol. 28, No. 2, pp. 247-249.

Clarke, R. (1968). A statistical theory of mobile radio reception, *Bell Systems Technical Journal*, Vol. 47, pp. 957-1000.

COST 207 TD(86) 51-REV 3 (WG1) (1986): "Proposal on channel transfer functions to be used in GSM tests late 1986", September 1986.

Dent, P., Bottomley, G.E., and Croft, T. (1993), Jakes fading model revisited, *IEE Electronics Letters*, Vol. 29, No. 13, pp. 1162-1163.

Deschamps, G.A. (1972). Ray techniques in electromagnetics, *Proceedings of the IEEE*, Vol. 60, pp. 1022-1035.

Dixit, S. (2006). On fixed-mobile network convergence, *Wireless Personal Communications*, Vol. 38, No. 1, pp. 55-65.

Ertel, R.B., Cartieri, P., Sowerby, K.W., Rappaport, T.S., and Reed, J.H. (1998). Overview of Spatial Channel Models for Antenna Array Communication Systems, *IEEE Personal Communications,* Vol. 5, No. 1, pp. 10-22.

Fourie, A., and Nitch, D. (2000). SuperNEC: antenna and indoor-propagation simulation program, *IEEE Antennas and Propagation Magazine*, Vol. 42, No. 3, 31-48.

Fusco, M. (1990). FDTD algorithm in curvilinear coordinates, *IEEE Transactions on Antennas and Propagation*, Vol. AP-38, pp. 76-88.

Ganesh, R., and Pahlavan, K. (1989). On arrival of paths in fading multipath indoor radio channels, *IEE Electronics Letters*, Vol. 25, No. 5, pp. 763-765.

Ganesh, R. (1991). *Time Domain Measurements, Modeling, and Simulation of the Indoor Radio Channel*. Ph.D. thesis, Worcester Polytechnic Institute.

GSM Recommendation 05.05 (1991). Radio transmission and reception, ETSI/PT, No. 12, January 1991.

Gudmundson, M. (1991). Correlation model for shadow fading in mobile radio systems, *Electronics Letters*, Vol. 27, No. 23, pp. 2145-2146.

Hansen, F., and Meno, F. I. (1977). Mobile fading – Rayleigh and lognormal superimposed, IEEE Transactions on Vehicular Technology, vol. VT-26, no. 4, pp. 332-335.

Harms, P.H., Lee, J.F., and Mittra, R. (1992). A study of the non-orthogonal FDTD method versus the conventional FDTD technique for computing resonant frequencies of cylindrical cavities, *IEEE Transactions on Microwave Theory and Techniques*, Vol. MTT-40, pp. 741-746.

Harada, H., and Prasad, R. (2002). *Simulation and Software Radio for Mobile Communications,* Artech House, Norwood, MA, USA.

Hashemi, H. (1993). Impulse response modeling of indoor radio propagation channels, *IEEE Journal on Selected Areas in Communications*, Vol. 11, pp. 967-978.

Hashemi, H., and Tholl, D. (1994). Statistical Modeling and Simulation of the RMS Delay Spread of Indoor Radio Propagation Channels, *IEEE Transaction on Vehicular Technology*, Vol. 43, No. 1, pp. 110-120.

Hata, M., and Nagatsu, T. (1980). Mobile location using signal strength measurements in cellular systems, *IEEE Transactions on Vehicular Technology*, Vol. 29, No. 2, pp. 245-251.

Holland, R. (1983). Finite difference solutions of Maxwell's equations in generalized non-orthogonal coordinates, *IEEE Transactions on Nuclear Science*, Vol. NS-30, No. 6, pp. 4589-4591.

Holt, T., Pahlavan, K., and Lee, J.F. (1992). A graphical indoor radio channel simulator using 2D ray tracing, *Proceedings of the PIMRC '92*, Boston, USA, pp. 411-416.

Howard, J.S., *Frequency Domain Characteristic and Autoregressive Modeling of the Indoor Radio Channel*. Ph.D. Thesis, Worcester Polytechnic Institute, Worcester MA.

Ikegami, F., Takeuchi, T., and Yoshida, S. (1991). Theoretical prediction of mean field strength for urban mobile radio, *IEEE Transactions on Antennas and Propagation*, Vol. 39, pp. 229-302.

International Telecommunication Union (ITU), "NGN Working Definition", available at http://www.itu.int/ITU-T/studygroups/com13/ngn2004/working_definition.html .

Jakes, W.C. (1974). *Microwave Mobile Communications*. Wiley, New York.

Jakes, W.C. (1994). *Microwave Mobile Communications*. IEEE Press.

Jeruchim, M.C., Balaban, P., and Shanmugan, K.S. (1992). *Simulation of Communication Systems*. Plenum Press, New York.

Joint Technical Committee of Committee T1 R1P1.4 and TIA TR46.3.3/TR45.4.4 on Wireless Access (1994). Final Report on RF Channel Characterization, No. JTC(AIR)/94.01.17-238R4, January 1994.

Karadimas, P., and Kotsopoulos, S.A. (2007). A modified Loo model with sectored and three dimensional multipath scattering, *World Wireless Congress 2007*, San Francisco, May 2007.

Karagiannidis, G.K., Zogas, D.A., Sagias, N.C., Kotsopoulos, S.A., and Tombras, G.S. (2005). Equal-gain and maximal-ratio combining over nonidentical Weibull fading channels, *IEEE Transactions on Wireless Communications*, Vol. 4, No. 3, pp. 841-846.

Kein, A., and Mohr, W. (1996). A statistical wideband mobile radio channel model including the direction of arrival, *IEEE 4th International Symposium on Spread Spectrum Techniques and Applications*, pp. 102-106.

Kim, S.C., Bertoni, H.L., Stern, M. (1996). Pulse Propagation Characteristics at 2.4GHz Inside Buildings, *IEEE Transactions on Vehicular Technology*, Vol. 45, No. 3, pp. 579-592.

Kotsopoulos, S.A., and Karagiannidis, G. (2000). Error Performance for Equal-gain Combiners over Rayleigh Fading Channels, *Journal of IEE Electronics Letters*, Vol.36, No. 10, pp. 892-894.

Lawton, M.C., Davies, R.L., and McGeehan, J.P. (1991). A ray launching method for the prediction of indoor radio channel characteristics, *PIMRC '91*, pp. 104-108, London, UK.

Lawton, M.C., and McGeehan, J.P. (1992). The application of GTD and ray launching techniques to channel modeling for cordless radio systems, *Proceedings of the 42nd IEEE Vehicular Technology Conference*, pp. 125-130, Denver, USA.

Lebherz, M., Wiesbeck, W., Blasberg, H.-J., and Krank, W. (1989). Calculation of broadcast coverage based on a digital terrain model, *Proceedings of the 1989 IEEE International Conference on Antennas and Propagation*, Vol. 2, pp. 355-359.

Lebherz, M., Wiesbeck, W., and Krank, W. (1992). A versatile wave propagation model for the VHF/UHF range considering three-dimensional terrain, *IEEE Transactions on Antennas and Propagation*, Vol. 40, pp. 1121-1131.

Lee, W.C.Y. (1982). *Mobile Communications Engineering*, McGraw Hill, New York.

Lee, W.C.Y. (1986). *Mobile Communications Design Fundamentals*, Sams, Indianapolis, IN.

Lee, J.F. (1993). Numerical solutions of TM scattering using an obliquely Cartesian finite difference time domain algorithm, *IEE Proceedings H: Microwaves, Antennas and Propagation*, Vol. 140, No. 1, pp. 23-28, February 1993.

Liang, G., Bertoni, H.K. (1998). A New Approach to 3-D Ray Tracing for Propagation Prediction in Cities, *IEEE Transactions on Antennas and Propagation*, Vol. 46, No. 6, pp. 853-863.

Liberti, J.C.Jr., and Rappaport, T.S. (1996). A geometrically based model for line-of-sight multipath radio channels, *Proceedings of the 46th IEEE Vehicular Technology Conference*, Vol. 2, pp. 844-848.

Liberti, J.C.Jr., and Rappaport, T.S. (1999). *Smart Antennas for Wireless Communications: IS-95 and Third Generation CDMA Applications*. Prentice Hall PTR, New Jersey.

Loo, C. (1985). A statistical model for a land mobile satelite link, IEEE Transactions on Vehicular Technology, vol. VT-34, no. 3, pp. 122-127.

Lotter, M.P., and van Rooyen, P. (1999). Cellular channel modeling and the performance of DS-CDMA systems with antenna arrays, *IEEE Journal on Selected Areas on Communications*, Vol. 17, No. 12, pp. 2181-2196.

Lu, M., Lo, T., and Litva, J. (1997). A physical spatio-temporal model of multipath propagation channels, *Proceedings of the 47th IEEE Vehicular Technology Conference*, pp. 180-184.

McKown, J.W., and Hamilton, R.L.Jr. (1991). Ray tracing as a design tool for radio networks, *IEEE Network Magazine*, Vol. 6, No. 6, pp. 27-30.

McPherson, G. (1990). *Statistics in Scientific Investigation*, Springer.

Mitilineos, S.A., Varlamos, P K., and Capsalis, C.N. (2004). A simulation method for bit error rate performance estimation for arbitrary angle of arrival channel models, *IEEE Antennas and Propagation Magazine*, Vol. 46, No. 2, pp. 158-163.

Mitilineos, S.A., Panagiotou, S.C., Varlamos, P.K., and Capsalis, C.N. (2005). Indoor environments propagation simulation using a hybrid MoM and UTD electromagnetic method, *Annals of Telecommunications*, Vol. 60, No. 9-10, pp.1231-1243.

Norklit, O., and Anderson, J.B. (1994). Mobile radio environments and adaptive arrays, *IEEE International Symposium on Personal, Indoor and Mobile Radio Communications (PIMRC)*, pp. 725-728.

O'Brien, W.M., Kenny, E.M., and Cullen, P.J. (2000). An Efficient Implementation of a Three-Dimensional Microcell Propagation Tool for Indoor and Outdoor Urban Environments, *IEEE Transactions on Vehicular Technology*, Vol. 49, No. 2, pp. 622-630.

Oestges, C., Clerck, B., Raynaud, L., and van Hoenacker, J.D. (2002). Deterministic Channel Modeling and Performance Simulation of Microcellular Wide-Band Communication Systems, *IEEE Transactions on Vehicular Technology*, Vol. 51, No. 6, pp. 1422-1430.

Okumura, Y., Ohmuri, E., Kawano, T., and Fukuda, K. (1968). Field strength and its variability in VHF and UHF land mobile radio service, *Rev. of the ECL*, Vol. 16, pp 825-873.

Ossana, J.Jr. (1964). A model for mobile radio fading due to building reflections: theoretical and experimental fading waveform power spectra, *Bell Systems Technical Journal*, Vol. 43, No. 6, pp. 2935-2971.

Pahlavan, K., Ganesh, R., and Hotaling, T. (1989). Multipath propagation measurements on manufacturing floors at 910MHz, *IEE Electronics Letters*, Vol. 25, No. 3, pp. 225-227.

Pahlavan, K., and Levesque, A.H. (1995). *Wireless Information Networks*. John Wiley & Sons, New York.

Papamichael, V., Soras, C., and Makios, V. (2003). FDTD Modeling and Characterization of the Indoor Radio Propagation Channel in the 434 MHz ISM Band, *ICECom 2003, 17th International Conference on Applied Electromagnetics and Communications*, pp. 217-220.

Paulraj, A., Nabar, R., and Gore, D. (2003). *Introduction to Space-Time Wireless Communications*. Cambridge University Press.

Polydorou, D.S., and Capsalis, C.N. (1997). A new theoretical model for the prediction of rapid fading variations in an indoor environment, *IEEE Transactions on Vehicular Technology*, Vol. 46, No. 3, pp. 748-754.

Pop, M.F., and Beaulieu, N.C. (1999). Statistical investigation of sum-of-sinusoids fading channel simulators, *GLOBECOM '99*, Vol. 1A, pp. 419-426, Rio de Janeiro, Brazil.

Pop, M.F., and Beaulieu, N.C. (2001). Limitations of sum-of-sinusoids fading channel simulators, *IEEE Transactions on Communications*, Vol. 49, No. 4, pp. 699-708.

Pop, M.F., and Beaulieu, N.C. (2002). Design of wide-sense stationary sum-of-sinusoids fading channel simulators, *Proceedings of th3 2002 IEEE International Conference on Communications*, Vol. 2, pp. 709-716.

Preston, S.L., Thiel, D.V., Smith, T.A, O'Keefe, S.G., and Lu, J.W. (1998). Base-station tracking in mobile communications using a switched parasitic antenna array, *IEEE Transactions on Antennas and Propagation*, Vol. 46, No. 6, pp. 841-844.

Raleigh, G.G., and Paulraj, A. (1995), "Time varying vector channel estimation for adaptive spatial equalization", *Proceedings of the 1995 IEEE GLOBECOM*, pp. 218-224.

Rappaport, T.S. (1989). Characterization of UHF multipath radio channels in factory building, *IEEE Transactions on Antennas and Propagation*, Vol. 37, No. 8, pp. 1058-1069.

Rappaport, T.S., Seidel, S.Y., and Takamizawa, K. (1991). Statistical channel impulse response models for factory and open plan building radio communication system design, *IEEE Transactions on Communications*, Vol. COM-39, No 5, pp. 794-806.

Rappaport, T.S., and Hawbaker, D.A. (1992). A ray tracing technique to predict path loss and delay spread inside buildings, *Proceedings of the 1992 IEEE GLOBECOM*, pp. 649-653.

Rappaport, T.S., Huang, W., and Feuerstein, M.J. (1993). Performance of decision feedback equalizers in simulated urban and indoor radio channels, *IEICE Transactions on Communications*, Vol. E76-B, No. 2.

Rizk, K., Wagen, J.F., Gardiol, F. (1997). Two-Dimensional Ray-Tracing Modeling for Propagation Prediction in Microcellular Environments, *IEEE Transactions on Vehicular Technology*, Vol. 46, No. 22, pp. 508-518.

Rossi, J.-P., and Levy, A.J. (1993). Propagation analysis in cellular environment with the help of models using ray theory and GTD, *Proceedings of the 43rd IEEE Vehicular Technology Conference*, pp. 253-256.

Ruggieri, M. (2006). Next generation of wired and wireless networks: the NavCom integration, *Wireless Personal Communications*, Vol. 38, No. 1, pp. 79-88.

Rustako, A.J., Amitay, N.Jr., Owens, G.J., and Roman, R.S. (1991). Radio propagation at microwave frequencies for line-of-sight microcellular mobile and personal communications, *IEEE Transactions on Vehicular Technology*, Vol. 40, pp. 203-210.

Sagias, N.C., Karagiannidis, G.K., Zogas, D.A., Tombras, G.S., and Kotsopoulos, S.A. (2005). Average output SINR of equal-gain diversity in correlated Nakagami-m fading with cochannel interference, *IEEE Transactions on Wireless Communications*, Vol. 4, No. 4, pp. 1407-1411.

Saleh, A.A.M., and Valenzuela, R.A. (1987). A statistical model for indoor multipath propagation, *IEEE Journal on Selected Areas in Communications*, Vol. SAC-5, No. 2, pp. 128-137.

Sarkar, T.K., Ji, Z., Kim, K., Medouri, Z., and Salazar-Palma, M. (2003). A survey of various propagation models for mobile communication, *IEEE Antennas and Propagation Magazine*, Vol. 45, No. 3, 51-82.

Schlub, R., Thiel, D.V., Lu, J.W., and O' Keefe, S.G. (2000). Dual-band switched parasitic wire antennas for communications and direction finding, *Proceedings of the 2000 IEEE Asia-Pacific Microwave Conference*, pp. 74-78, Sydney, Australia.

Seidel, S.Y., and Rappaport, T.S. (1994). Site-specific propagation prediction for wireless in-building personal communication system design, *IEEE Transactions on Vehicular Technology*, Vol. 43, No. 4, pp. 879-891.

Sibille, A., Roblin, C., and Poncelet, G. (1997). Circular switched monopole arrays for beam steering wireless communications," *Electronics Letters*, Vol. 33, No. 7, pp. 551-552.

Son, H.W., and Myung, N.H. (1999). A deterministic ray tube method for microcellular wave propagation prediction model, *IEEE Transactions on Antennas and Propagation*, Vol. 47, No. 8, pp. 1344-1350.

Stapleton, S.P., Carbo, X., and McKeen, T. (1994). Spatial channel simulator for phased arrays, *IEEE 44th Vehicular Technology Conference*, Vol. 3, pp. 1789-1792, Stockholm, Sweden.

Stapleton, S.P., Carbo, X., and McKeen, T. (1996). Tracking and diversity for a mobile communications base station array antenna", *IEEE 46th Vehicular Technology Conference*, Vol. 3, pp. 1695-1699, Atlanta, GA, USA.

Stuber, G.L. (2001). *Principles of Mobile Communication*. Kluwer Academic Publisher.

Suzuki, H. (1977). A statistical model for urban radio propagation: multipath characteristics in New York city, *IEEE Transactions on Communications*, Vol. 25, pp. 673-680.

Taflove, A., and Morris, M.E. (1975). Numerical solution of steady-state electromagnetic scattering problems using the time-dependent Maxwell's equations, *IEEE Transactions on Microwave Theory and Techniques*, Vol. MTT-23, pp. 623-630.

Talbi, L. (2001). Simulation of Indoor UHF Propagation Using Numerical Technique, *Canadian Conference on Electrical and Computer Engineering*, Vol. 2, pp. 1357-1362.

Tillman, J.D., Jr. (1966). *The Theory and Design of Circular Antenna Arrays*. University of Tennessee Engineering Experimental Station.

Toumbakaris, D., and Kotsopoulos, S.A. (2007). Delay-constrained transmission over flat fading channels in the low SNR range, *18th Annual IEEE International Symposium on Personal, Indoor and Mobile Radio Communications*, Athens, Greece, 3-7 September 2007, to be published.

Turin, G.L., Clapp, F.D., Johnston, T.L., Fine, S.B., and Lavry, D. (1972). A statistical model of urban multipath propagation, *IEEE Transactions on Vehicular Technology*, Vol. 21, No. 1, pp. 1-9.

Varlamos, P.K., and Capsalis, C.N. (2003). Design of a six-sector switched parasitic planar array using the method of genetic algorithms, *Wireless Personal Communications*, Vol. 26, No. 1, pp. 77-88.

Varlamos, P.K., Mitilineos, S.A., and Capsalis, C.N. (2006). Diversity performance of a switched parasitic circular array in an indoor multipath environment, *Proceedings of the European Microwave Association (EuMA),* to be published, September 2006.

Vellis, F.E., and Capsalis, C.N. (2000). A model for the statistical characterization of fast fading in the presence of a user, *Wireless Personal Communications*, Vol. 15, pp. 207-219.

Wallace, J.W., and Jensen, M.A. (2003). Validation of Parametric Directional MIMO Channel Models from Wideband FDTD Simulations of a Simple Indoor Environment, *IEEE 2003 Antennas and Propagation Society International Symposium*, Vol. 2, pp. 535-538.

Yang, G., Li, S., Lee, J.F., and Pahlavan, K. (1993). "Computer simulation of indoor radio propagation, *IEEE 1993 International Symposium on Personal, Indoor and Mobile Radio Communication*, Yokohama, Japan.

Yang, G., Pahlavan, K., and Lee, J.F. (1993). A 3D propagation model with polarization characteristics in indoor radio channels, *Proceedings of the 1993 IEEE GLOBECOM*, Vol. 2, pp. 1252-1256, Houston, USA.

Yang, C.F., Wu, B.C., and Ko, C.J. (1998). A Ray-Tracing Method for Modeling Indoor Wave Propagation and Penetration, *IEEE Transactions on Antennas and Propagation*, Vol. 46, No. 6, pp. 907-919.

Yee, K.S. (1966). Numerical solution of initial boundary value problems involving Maxwell's equations in isotropic media, *IEEE Transactions on Antennas and Propagation*, Vol. AP-14, pp. 302-307.

Yegani, P., and McGillem, C.D. (1991). A statistical model for the factory radio channel, *IEEE Transactions on Communications*, Vol. 39, pp. 1445-1454.

Zetterberg, P. (1995). *Mobile Communication with Base Station Antenna Arrays: Propagation Modeling and System Capacity*. Master Thesis, Royal Institute of Technology, Stockholm, Sweden.

Zetterberg, P., Espensen, P.L., and Mogensen, P. (1996). Propagation, beamsteering and uplink combining algorithms for cellular systems, *Proceedings of the 1996 ACTS Mobile Communications Summit*, pp. 500-509, Granada, Spain.

Zhang, W. (1997). A Wide-Band Propagation Model Based on UTD for Cellular Mobile Radio Communications, *IEEE Transactions on Antennas and Propagation*, Vol. 45, No. 11, pp. 1669-1678.

KEY TERMS

Deterministic Channel Models: Channel models based on (usually digital) architectural plans or topographical maps of the propagation environment.

Empirical Channel Models: Channel models based on in-situ channel measurements.

Frequency Flat Fading: A type of small scale fading where all frequency signal components experience the same magnitude of fading; corresponds to the case where the signal bandwidth is smaller than the channel coherence bandwidth.

Frequency Selective Fading: A type of small scale fading where different frequency signal components therefore experience decorelated fading; corresponds to the case where the signal bandwidth is larger than the channel coherence bandwidth.

Geometric Channel Models: Channel models based on abstract geometric characteristics of the propagation environment.

Mobile Channel: A wireless communications propagation description, referring to mobile receivers and/or transmitters.

Simulation: Artificial Reality, i.e. the research field whose intention is to mimic one or more attributes of reality.

Smart Antennas: Antenna arrays that are capable of automatically controling each element's gain and phase, thus delivering optimal or sub-optimal radiation patterns with respect to a desired evaluation criterion.

Small Scale Fading: Severe signal strength fluctuations within distances in the order of wavelength.

Statistical Channel Models: Channel models based on given probability density functions of channel characteristics.